Funnel-based output tracking control for nonlinear impulsive switched systems

Atiyeh Karimi Pour[a,b], Stephan Trenn[b,*], Moosa Ayati[a,*], Mohammad Reza Zakerzadeh[a]

[a] *School of Mechanical Engineering, College of Engineering, University of Tehran, P.O.B. 11155-4563, Tehran, Iran*
[b] *Bernoulli Institute for Mathematics, CS, and AI, University of Groningen, Nijenborgh 9, Groningen, 9747 AG, The Netherlands*

Abstract

We study output tracking for nonlinear impulsive switched systems with global relative degree one under prescribed performance requirements. Classical funnel control is not directly applicable in this setting, since output jumps can cause violations of funnel constraints. To address this, we design an adjusted funnel boundary that contracts prior to jumps and expands afterward, computed offline based on the stability of the internal dynamics and bounded jump maps. We also derive sufficient conditions ensuring bounded control input. To obtain tighter bounds, practical ISS is employed in place of BIBO stability, yielding smaller input requirements. Additional refinements include asymmetric jump bounds, level-set adjustments, and real-time funnel adaptation, which further improve performance. Numerical examples confirm stability and practical tracking under disturbance impulses and switching.

Keywords: Funnel control, Impulsive Switched systems, Output tracking, Nonlinear control

1. Introduction

We consider the output tracking problem for a nonlinear single-input single-output (SISO) impulsive switched system with global relative degree one. We assume that the system dynamics can be described by:

$$\begin{aligned} \dot{y}(t) &= f_{\sigma(t)}(y(t), z(t)) + g_{\sigma(t)}(y(t), z(t)) \cdot u(t), && t \neq t_k, \\ y(t_k^+) &= J_{\sigma(t_k^+)}(y(t_k^-), z(t_k^-)), && t = t_k, \\ \dot{z}(t) &= f^{\mathrm{z}}_{\sigma(t)}(y(t), z(t)), && t \neq t_k, \\ z(t_k^+) &= J^{\mathrm{z}}_{\sigma(t_k^+)}(y(t_k^-), z(t_k^-)), && t = t_k, \\ y(t_0^+) &= y_0 \in \mathbb{R},\ z(t_0^+) = z_0 \in \mathbb{R}^{n-1}. \end{aligned} \tag{1}$$

- $y : \mathbb{R}_{\geq 0} \to \mathbb{R}$ denotes the system output.
- $z : \mathbb{R}_{\geq 0} \to \mathbb{R}^{n-1}$ represents the internal state.
- $u : \mathbb{R}_{\geq 0} \to \mathbb{R}$ denotes the control input (to be designed).
- $\mathcal{T} = \{t_k \mid k \in \mathbb{N}, t_k \in \mathbb{R}_{\geq 0}, t_k - t_{k-1} > 0\}$ is the impulse time sequence, where $t_0 := 0$ and $t_k \to \infty$ as $k \to \infty$.
- $\sigma : \mathbb{R}_{\geq 0} \to \Sigma := \{1, 2, \ldots, \mathrm{M}\}$ is the switching signal, specifying the active mode of the system at t.
- The functions $(f_{\mathrm{m}}, g_{\mathrm{m}}) : \mathbb{R} \times \mathbb{R}^{n-1} \to \mathbb{R}$ and $f^{\mathrm{z}}_{\mathrm{m}} : \mathbb{R} \times \mathbb{R}^{n-1} \to \mathbb{R}^{n-1}$, $\mathrm{m} \in \Sigma$, describe the system's behavior during continuous evolution, and are assumed to be locally Lipschitz.
- $J_{\mathrm{m}} : \mathbb{R} \times \mathbb{R}^{n-1} \to \mathbb{R}$ and $J^{\mathrm{z}}_{\mathrm{m}} : \mathbb{R} \times \mathbb{R}^{n-1} \to \mathbb{R}^{n-1}$ characterize the discrete jump maps in the output and internal states at impulse instances.[1]the implementation of our proposed controller does not require explicit knowledge of that coordinate transformation. Note that even if no jumps occur in $(*)$, the coordinate transformation leading to (1) is generally mode-dependent, introducing state jumps in the internal states. The switching nature of the output map in $(*)$ also induces output jumps in (1).

The objective is to design a control input $u(t)$ such that the system output $y(t)$ tracks a given reference trajectory $y^{\mathrm{r}} : \mathbb{R}_{\geq 0} \to \mathbb{R}$, while ensuring that the tracking error ideally remains within a prescribed, time-varying desired boundary. Specifically, we define the tracking error as

$$e(t) = y(t) - y^{\mathrm{r}}(t), \tag{2}$$

and ideally aim to enforce the constraint

$$|e(t)| < \psi^{\mathrm{d}}(t), \quad \forall t \geq 0, \tag{3}$$

where $\psi^{\mathrm{d}} : [0, \infty) \to \mathbb{R}_{>0}$ is a smooth function that defines the desired funnel boundary (Fig. 1).

Due to impulsive effects, the tracking error $e(t)$ cannot be guaranteed to remain within the desired funnel $\psi^{\mathrm{d}}(t)$

*Corresponding authors
Email addresses: s.trenn@rug.nl (Stephan Trenn), m.ayati@ut.ac.ir (Moosa Ayati)

[1] Our approach also works without change for nonlinear impulsive switched system in the general form

$$\begin{aligned} \dot{x}(t) &= F_{\sigma(t)}(x(t), u(t)), && t \neq t_k, \\ x(t_k^+) &= E_{\sigma(t)}(x(t_k^-)), && t = t_k, \\ y(t) &= H_{\sigma(t)}(x(t)), \end{aligned} \tag{$*$}$$

provided that there exists a nonlinear state-space coordinate transformation that converts the system into the relative-degree one Byrnes-Isidori form (1) (cf.[1, Thm. 13.1]);

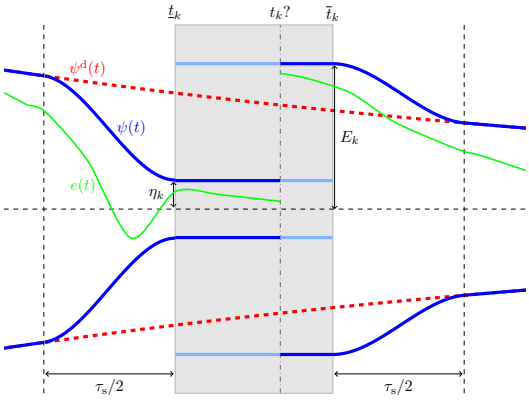

Figure 1: Schematic of the adjusted funnel $\psi(t)$. The gray area represents the jump uncertainty window. The light blue lines at levels η_k and E_k represent parallel boundaries that are both reserved throughout the jump window prior to the experiment.

after jumps. To address this, we exploit prior knowledge of jump bounds to compute the maximum possible error increase and, based on this, construct an extended funnel boundary $\psi(t)$ offline, independent of the closed-loop dynamics. After a jump, the error is allowed to temporarily enter this extended funnel, while a recovery mechanism ensures that it returns to $\psi^{\mathrm{d}}(t)$ within a prescribed time interval. Thus, during normal operation the error remains inside $\psi^{\mathrm{d}}(t)$, but immediately after jumps it may transiently lie in $\psi(t)$. Figure 1 illustrates this approach.

Impulsive switched systems arise in diverse applications, including robotics [2], power systems [3], neural networks [4], and communication networks [5]. Prior research has focused on topics such as stability under switching [6, 7, 8], observability [9, 10, 11, 12], and robustness [13]. To the best of our knowledge, however, funnel control has not been investigated for impulsive switched systems with output jumps.

Funnel control was first introduced in 2002 by Ilchmann et al. [14] for nonlinear systems with relative degree one, subject to bounded disturbances and uncertainties. Since then, it has been extended to address a wide range of systems, including functional differential equations [15], those with higher relative degrees [16], input constraints [17, 18], systems with non-minimum phase internal dynamics [19], infinite-dimensional systems [20], multi-agent systems [21, 22, 23], and systems with unmatched uncertainties with possible discontinuous functions [24]. For a comprehensive survey of funnel controllers, see Berger et al. [25].

The funnel controller is an adaptive high-gain output-feedback scheme that ensures output tracking using only output measurements, under minimal structural assumptions: having a well-defined relative degree, BIBO-stable internal dynamics, and known input-channel sign.

Therefore, funnel control offers distinct advantages over comparable tracking methods. Unlike control barrier functions [26], it does not require full-state information or feedback linearization. Prescribed-performance control (PPC) also shapes transients through performance functions, but most classical PPC designs are more model-dependent and assume full-state availability [27], while output-feedback variants typically require observers [28]. Output-only implementations exist, though at the cost of additional structural layers and assumptions [29]. A brief overview of the classical funnel control framework is provided in Section 2.

However, classical funnel controllers are not applicable to impulsive switched systems, since output jumps at impulse times can drive the error outside the funnel, making the controller ill-defined.

We therefore introduce an adjusted funnel controller tailored to impulsive switched systems. In addition to the assumptions of classical funnel control, it requires limited structural knowledge: the jump windows are assumed known, while the exact jump instances remain unknown. The jump maps themselves are not required, only bounds on their effects. Accordingly, the funnel boundary $\psi(t)$ is contracted prior to each window, widened during it to accommodate worst-case error growth, and smoothly restored to the desired boundary afterward.

Berger and Lanza [30] address output dropouts via an availability function: during loss intervals the input is set to zero, and upon reappearance a shifted base funnel is applied. Their approach widens the funnel without bound during each loss interval and always restarts from a fixed design. By contrast, our method handles jump events and differs in several key respects: the funnel is pre-shrunk to mitigate post-jump error, two concurrent boundaries are maintained with widening triggered only at jump occurrences, the required expansion is computed per jump window with boundedness guarantees, and this expansion is further refined online using information from past jumps. A preliminary version of these results appeared in [31], but without addressing whether the adjusted funnel boundary remains bounded. This issue is crucial, since in impulsive systems the interaction between internal states and output jumps can lead to instability even when the internal states are individually stable. The following example illustrates this point. Consider the nonlinear system:

$$\begin{aligned} \dot{y}(t) &= -z(t)y(t) - y(t), && t \notin t_k, \\ y(t_k^+) &= 2z(t_k^-), && t = t_k, \\ \dot{z}(t) &= -\mu z(t) + y(t)^2, \end{aligned} \tag{4}$$

where $(y(0), z(0)) = (5, 5)$ and $\mu \geq 0$, and periodic impulses occur at $t_k = 2k$, $k \in \mathbb{N}$.

This system *without impulses* is globally stable with the Lyapunov function $V(t) = \frac{1}{2}(y(t)^2 + z(t)^2)$. In fact, $\dot{V}(t) = y(t)\dot{y}(t) + z(t)\dot{z}(t) = -y(t)^2 - \mu z(t)^2 \leq 0$. Moreover, by expressing $\dot{V}(t) = -2\mu V(t) - y(t)^2(1-\mu)$, it follows that for $\mu \leq 1$, $\dot{V}(t) \leq -2\mu V(t)$.

Now, to assess the effect of the impulses, we have $V(t) \leq V(t_{k-1}^+)e^{-2\mu(t-t_{k-1})}$ for $t \in [t_{k-1}, t_k)$. Immediately after a jump, $V(t_{k-1}^+) = \frac{1}{2}(y(t_{k-1}^+)^2 + z(t_{k-1}^+)^2)$; using $y(t_{k-1}^+) =$

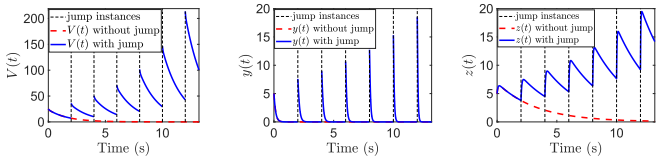

(a) (b) (c)

Figure 2: Successive increases in jump heights and the internal state norm in the system (4) with $\mu = 0.3$. (a) Lyapunov function. (b) Output. (c) Internal state.

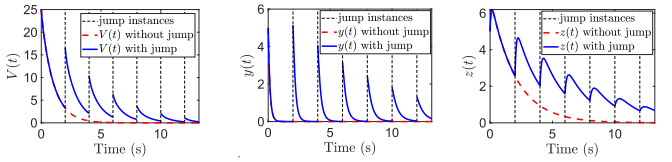

(a) (b) (c)

Figure 3: Non-increasing jump heights and the internal state norm in the system (4) with $\mu = 0.5$. (a) Lyapunov function. (b) Output. (c) Internal state.

$2z(t_{k-1}^-)$, we find $V(t_{k-1}^+) = \frac{5}{2}z(t_{k-1}^-)^2$. Combining this with the exponential decay between jumps, and knowing $z(t_{k-1}^-)^2 \le 2V(t_{k-1}^-)$, we derive:

$$\begin{aligned} V(t_k^-) &\le \frac{5}{2}z(t_{k-1}^-)^2 e^{-2\mu(t_k - t_{k-1})} \\ &\le 5V(t_{k-1}^-)e^{-2\mu(t_k - t_{k-1})}. \end{aligned} \tag{5}$$

Unrolling this recursion gives $V(t_k^-) \le \frac{1}{5}V(0)(5e^{-4\mu})^k$. For $\mu = 0.3$, $V(t_k^-) \le \frac{1}{5}V(0)(1.51)^k$, demonstrating unbounded growth of the upper bound of the system energy despite the system's inherent stability. Fig. 2a, confirms this behavior, as $V(t_k^-)$ diverges due to the impulses. This analysis shows that instability arises from the interaction between the output and the internal states: growth in $y(t)$ amplifies $z(t)$, which in turn increases the impulse magnitude, leading to divergence over time (see Figs. 2b–2c). In this case, any adjusted funnel inevitably grows unbounded.

However, this interplay does not *always* cause instability. As shown in (5), longer dwell times $(t_k - t_{k-1})$ or more stable internal dynamics (larger μ) can preserve stability. For instance, with $\mu = 0.5$ we obtain

$$V(t_k^-) \le \tfrac{1}{5}V(0)(0.68)^k, \quad \forall k,$$

demonstrating exponential decay of the system energy. The corresponding trajectories of $V(t)$, $y(t)$, and $z(t)$ are shown in Fig. 3.

These observations naturally lead to the central question: how can the combined effect of internal-state dynamics and output jumps be systematically characterized to assess stability in impulsive switched tracking problems?

To address this, we define a map that captures the interplay between the internal states and the output, enabling us to derive sufficient conditions for ensuring a bounded adjusted funnel and bounded control inputs. We demonstrate that systems with a mix of stable and unstable modes—such as those in the example (4) with $\mu = 0.5$ and $\mu = 0.3$, respectively—can still achieve bounded performance. Based on this analysis, we determine a quantitative upper bound for the control input required to return the error to the desired funnel.

To further enhance performance, we replace the classical BIBO stability assumption of the internal dynamics, commonly used in classical funnel controllers, with a practical input-to-state stability (ISS) assumption. This modification significantly improves the adjusted funnel bounds. Under the practical ISS assumption, we also provide sufficient conditions on the impulse time sequences to guarantee bounded adjusted funnel and control input for multi-mode systems.

Finally, to further refine the adjusted funnel bounds, we propose three other strategies: (1) asymmetric jump bounds, resulting in asymmetric funnel boundaries; (2) the level-set method, which precomputes error levels to mitigate the error growth during experiments; and (3) real-time funnel adaptation, which dynamically adjust the funnel boundary based on actual output and post-jump error values.

The main contributions are:

- Output-tracking control for relative-degree-one nonlinear switched systems subject to disturbance jumps, under prescribed performance requirements.
- Sufficient conditions for bounded control input under disturbance jumps, including explicit quantitative bounds.
- Extension of the framework to ISS internal dynamics (instead of BIBO), yielding tighter input bounds.
- Conditions on impulse-time sequences that ensure bounded inputs while maintaining tracking performance under disturbance jumps.
- Real-time performance enhancement using measured output data.

The paper is organized as follows: In Section 2, classical funnel control is reviewed and afterwards the content is split into two main parts. Part I develops the foundations of the adjusted funnel framework, including adjusted funnel construction (Section 3), boundedness conditions for the adjusted funnel (Section 4), and quantitative bounds on the control input (Section 4.2). Part II introduces refinement strategies that further tighten the funnel boundary, including an extension to practical ISS-stable internal dynamics (instead of BIBO stability), which substantially improves both the funnel boundary and the control-input bound (Section 5). Additional refinements include asymmetric jump maps and real-time funnel boundary adaptation (Section 6). The paper concludes with a summary and outlook (Section 7). Numerical examples are provided throughout to illustrate the results.[2]

[2]The MATLAB implementation of the proposed controller is

2. Preliminaries: Classical Funnel Controllers

In this section, we review the classical funnel control framework, which is designed to achieve trajectory tracking for nonlinear systems with relative degree one. Foundational works include the introduction of performance funnels in [14] and their rigorous analysis in [15],

Consider a nonlinear system:

$$\begin{aligned}\dot{x}(t) &= F(x(t), u(t)), \quad x(0) = x_0,\\ y(t) &= H(x(t)),\end{aligned}$$

where: $x(t) \in \mathbb{R}^n$ is the state vector, $u(t) \in \mathbb{R}$ is the control input, $y(t) \in \mathbb{R}$ is the system output. Additionally, $F : \mathbb{R}^n \times \mathbb{R} \to \mathbb{R}^n$ and $H : \mathbb{R}^n \to \mathbb{R}$ are assumed to be locally Lipschitz mappings.

Suppose there exists a smooth, nonlinear coordinate transformation $x \mapsto (y, z)$ such that the system can be written in Byrnes–Isidori normal form for relative degree one systems:

$$\dot{y}(t) = f(y(t), z(t)) + g(y(t), z(t)) \cdot u(t), \tag{6a}$$
$$\dot{z}(t) = f^{\mathrm{z}}(y(t), z(t)), \tag{6b}$$

where $f, g,$ and f^{z} are assumed to be locally Lipschitz and $z(t) \in \mathbb{R}^{n-1}$ represents the internal states. Assume the following:

(A1) $g(y, z) > 0, \quad \forall\, y, z.$

(A2) The internal dynamics (6b) are BIBO stable. Specifically, for every bounded signal y and corresponding solution z of (6b) we have that

$$\|z(t)\| \leq b(\|z(t_0)\|, \|y_{[t_0,t)}\|_\infty), \quad \forall t \in [t_0, \infty),$$

for some continuous function b. Also, we assume that $z(t_0) \in Z_0$ for some bounded $Z_0 \in \mathbb{R}^{n-1}$.

Remark 2.1. *Classical funnel controllers treat explicit time-dependence of f and g as bounded disturbance terms [14, 16, 32]. Our framework* (systems (1), (6)) *can likewise accommodate such time-varying functions under the same boundedness assumption. For simplicity and to avoid additional notations, we restrict ourselves to the time-invariant case in the following.*

The goal is to design a control input $u(t)$ that ensures the error $e(t)$ strictly remains within the desired funnel, namely,

$$|e(t)| \leq \psi^{\mathrm{d}}(t) - \varepsilon, \quad \text{for some } \varepsilon > 0.$$

The surprisingly simple solution to achieve this goal is the funnel controller consisting of a simple (time-varying) proportional negative error feedback

$$u(t) = -k(t)e(t), \tag{7a}$$

together with the simple (non-dynamic) funnel gain

$$k(t) = \frac{1}{\psi^{\mathrm{d}}(t) - |e(t)|}. \tag{7b}$$

The intuition behind this controller design is that nonlinear systems equivalent to (6) possess a high-gain property: a sufficiently large proportional error feedback stabilizes the error dynamics. The funnel controller leverages this property by increasing the feedback gain as the error approaches the funnel boundary, thereby preventing constraint violation, while keeping the gain moderate when the error is well inside the boundary.

We now present the fundamental result for classical funnel controllers, which guarantees for any interval $[t_0, t_f)$ of interest, that if the initial error satisfies $|e(t_0)| < \psi^{\mathrm{d}}(t_0)$, the error remains strictly within the prescribed funnel for the complete interval $[t_0, t_f)$ and the left-limit values of all signals at t_f^- are well defined. While classical funnel controller focuses on the case $t_f = \infty$, we focus here on the case that t_f is finite, because in the context of impulsive systems, we analyze the closed loop behavior inductively from one jump instant to the next.

Lemma 2.2. *Consider a nonlinear system which is equivalent to (6) and suppose that assumptions **(A1)**–**(A2)** hold. Let $y^{\mathrm{r}} : [t_0, t_f] \to \mathbb{R}$ be a reference trajectory that is continuously differentiable, and let $\psi^{\mathrm{d}} : [t_0, t_f] \to (0, \infty)$ be a prescribed funnel boundary. If the initial error satisfies $|e(t_0)| < \psi^{\mathrm{d}}(t_0)$, then the control law defined in* (7) *guarantees the existence of $\varepsilon > 0$ such that the unique solution of the closed loop satisfies*

$$|e(t)| \leq \psi^{\mathrm{d}}(t) - \varepsilon, \quad \forall t \in [t_0, t_f).$$

In particular, all closed loop signals remain bounded on $[t_0, t_f)$ and have well-defined left-limits at t_f^-.

Proof. This is a simple consequence of the well established classical funnel controller [14]; however, for the sake of completeness we provide a proof-sketch here. Existence and uniqueness of a local solution $(y, z) : [t_0, \omega) \to \mathbb{R} \times \mathbb{R}^{n-1}$ to (6) for some $\omega \in [t_0, t_f)$ follow from the fact that, under the continuous feedback, the closed-loop vector field is locally Lipschitz in (y, z) on the set $\{|e| < \psi^{\mathrm{d}}(t)\}$ and that $|e(t_0)| < \psi^{\mathrm{d}}(t_0)$.

We will now show that there exists $C_1, C_2 \in \mathbb{R}$ and $\gamma > 0$ (defined independently of ω) such that for all $t \in [t_0, \omega)$ we have

$$\dot{e}(t) \begin{cases} \leq C_1 + \gamma u(t), & \text{if } u(t) < 0 \\ \geq C_2 + \gamma u(t), & \text{if } u(t) \geq 0 \end{cases} \tag{8}$$

Towards this goal, we first observe that $|e(t)| < \psi^{\mathrm{d}}(t)$ for all $t \in [t_0, \omega)$ (domain of the differential equation) and since the funnel and the reference signal are assumed to be bounded on $[t_0, t_f]$, we have that $y = y^{\mathrm{d}} + e$ is bounded on $[t_0, \omega)$, i.e. there exists $Y^{\min} < Y^{\max}$ (whose size is independent from ω) such that $y(t) \in [Y^{\min}, Y^{\max}]$ for all

available at Zenodo: `https://doi.org/10.5281/zenodo.15275315`.

$t \in [t_0, \omega)$. From assumption **(A2)**, it then follows that there exists $Z^{\max}$ (depending in $Y^{\min}, Y^{\max}$ and Z_0, but not on ω) such that $\|z(t)\| \leq Z^{\max}$ for all $t \in [t_0, \omega)$. Since f is continuous, we can define $F^{\max\,/\,\min} \in \mathbb{R}$ as the maximum/minimum of $f(y,z)$ considered on the compact domain $[Y^{\min}, Y^{\max}] \times \{z \in \mathbb{R}^{n-1} \mid \|z\| \leq Z^{\max}\}$; similarly we can define $G^{\min} > 0$ as the minimum of $g(y,z)$ on the same compact set. By observing that

$$\dot{e}(t) = \dot{y}(t) - \dot{y}^{\mathrm{r}}(t) = f(y,z) + g(y,z)u(t) - \dot{y}^{\mathrm{r}}(t),$$

we can now conclude that (8) holds with $C_1 := F^{\max} - \min_{t\in[t_0,t_f]} \dot{y}^{\mathrm{d}}(t)$, $C_2 := F^{\min} - \max_{t\in[t_0,t_f]} \dot{y}^{\mathrm{r}}(t)$ and $\gamma := G^{\min}$.

We will now show that for sufficiently small ε the (time-varying) region

$$\mathcal{F}_\varepsilon := \{(t,e) \mid |e(t)| \leq \psi^{\mathrm{d}}(t) - \varepsilon\}$$

is a positive invariant set for the error dynamics. Note that by assumption $\min_{t\in[t_0,t_f]} \psi^{\mathrm{d}}(t) := \underline{\psi^{\mathrm{d}}} > 0$, we have to assume in the following that $\varepsilon < \underline{\psi^{\mathrm{d}}}$ to ensure that $\mathcal{F}_\varepsilon$ is well defined (i.e. for all $t \in [t_0, t_f)$ we have that $(t,0)$ is in the interior of $\mathcal{F}_\varepsilon$).

Seeking a contradiction, we assume that there is a solution for which the error signal leaves $\mathcal{F}_\varepsilon$. Then there is a minimal $t_\varepsilon \in (t_0, \omega)$ such that $|e(t_\varepsilon)| = \psi^{\mathrm{d}}(t_\varepsilon) - \varepsilon$. In the following we will only consider the case $e(t^\varepsilon) > 0$; the other case follows completely analogous.

By (8) together with $u(t_\varepsilon) = -\frac{1}{\varepsilon} e(t_\varepsilon) \leq -\frac{\psi^{\mathrm{d}} - \varepsilon}{\varepsilon} < 0$, we then have

$$\dot{e}(t_\varepsilon) \leq C - \gamma \frac{\underline{\psi^{\mathrm{d}}} - \varepsilon}{\varepsilon} \to -\infty \text{ as } \varepsilon \to 0.$$

Let $\underline{d\psi^{\mathrm{d}}} := \min_{t\in[t_0,t_f]} \dot{\psi}^{\mathrm{d}}(t)$, then there exists $\varepsilon > 0$ (independent of ω) such that $\dot{e}(t_\varepsilon) \leq \underline{d\psi^{\mathrm{d}}} \leq \dot{\psi}^{\mathrm{d}}(t_\varepsilon)$. But this means that the error signal could not approach the boundary of $\mathcal{F}_\varepsilon$ from the inside, which shows that the error signal cannot leave $\mathcal{F}_\varepsilon$ for sufficiently small $\varepsilon > 0$.

Consequently, the solution (y,z) evolves within a compact domain, hence for a maximally extended solution it must hold that $\omega = t_f$. Furthermore, utilizing the above derived bounds for y and z, we can conclude that also $\dot{y}$ and $\dot{z}$ are bounded, whence $y(t_f^-)$ and $z(t_f^-)$ are well defined. □

Part I: Foundations of Adjusted Funnel Control

In this part, we establish the foundations of the proposed framework. We begin by constructing an adjusted funnel boundary for impulsive switched systems that accommodates output jumps. Next, we derive sufficient conditions ensuring that the adjusted funnel remains bounded, thereby guaranteeing bounded control input. Finally, we provide quantitative bounds on the control input in terms of the available prior information. In summary, Part I shows that, under the stated sufficient conditions, a nonlinear relative-degree-one impulsive switched system (1) can achieve output tracking via funnel control with an explicitly known bound on the control input.

3. Adjusted Funnel Controller Design

In this section, we introduce the assumptions and structural properties of the system. Based on these, we develop algorithms for constructing an *adjusted funnel boundary* tailored to impulsive switched systems. The main results are formalized in a theorem showing that, with this adjusted boundary, the tracking error remains within the funnel even in the presence of jumps.

Note that, for simplicity, x_i^+ and x_i^- are used to denote $x(t_i^+)$ and $x(t_i^-)$, respectively, where x represents a general variable.

3.1. Key Properties and Assumptions

The proposed controller, like any other funnel controller, operates without requiring precise knowledge of the system model, initial conditions, or detailed information about specific jump maps or instances. General structural assumptions about the system model and a basic understanding of the jumps are sufficient.

The structural assumptions for the relative degree one system described in (1) are formulated as follows.

(S1) For all y, z and $\mathrm{m} \in \Sigma$, $g_{\mathrm{m}}(y,z) > 0$.

(S2) The internal states of each mode are BIBO stable. Specifically, for all $t_k \leq s < t < t_{k+1}$, we have

$$\|z(t)\| \leq b_{\sigma(t)}\big(\|z(s^+)\|, \|y_{[s,t)}\|_\infty\big), \tag{9a}$$

where each mode $\mathrm{m} \in \Sigma$ has an associated known continuous function $b_{\mathrm{m}} : \mathbb{R}_{\geq 0} \times \mathbb{R}_{\geq 0} \to \mathbb{R}_{\geq 0}$. The variables t_k and t_{k+1} denote two consecutive jump instances. Note that the BIBO assumption will be sharpened later by a practical ISS assumption in the refinement section (Assumption **(S2)′**).

(S3) The initial conditions of the internal states, $z_0 = z(t_0^+)$, satisfy $z_0 \in Z_0$, where $Z_0 \subset \mathbb{R}^{n-1}$ is a bounded set with a known bound $Z_0^+ \geq \sup_{z\in Z_0} \|z\|$.

(S4) The switching signal $\sigma : \mathbb{R}_{\geq 0} \to \Sigma := 1, 2, \ldots, \mathrm{M}$ is a piecewise-constant, right-continuous function (i.e. $\sigma(t^+) = \sigma(t)$ for all t), whose set of discontinuities is contained in the impulse time sequence $\mathcal{T}$. While the exact switching times are not assumed to be known, the mode sequence $\{\sigma_k\}_{k\in\mathbb{N}_0}$, where $\sigma(t) = \sigma_k$ for all $t \in [t_k, t_{k+1})$, is assumed to be known.

There are some assumptions regarding prior information about jumps, which are specified below.

(J1) Exact knowledge of the jump instances t_k is not required. Instead, we assume access to a known interval $\mathcal{I}_k := [\underline{t}_k, \bar{t}_k]$ satisfying $t_k \in \mathcal{I}_k$. Throughout this paper, we refer to $\mathcal{I}_k$ as the jump window. Furthermore, it is assumed that for some known $\tau_s > 0$, we have that

$\underline{t}_{k+1} - \bar{t}_k \geq \tau_s$ (dwell time condition). For $k = 0$, we set $\bar{t}_0 := t_0 = 0$ and assume that no jump occurs at t_0.

(J2) The jump maps J_m and J^z_m for $\mathrm{m} \in \Sigma$ are unknown. However, we assume that the jump heights are bounded (not necessarily tight) by known smooth functions α_m and $\alpha^\mathrm{z}_\mathrm{m}$. Specifically:

$$|y_k^+ - y_k^-| = |J_{\sigma_k}(y_k^-, z_k^-) - y_k^-| \leq \alpha_{\sigma_k}(y_k^-, \|z_k^-\|) \quad (10a)$$

and

$$\|z_k^+\| = \|J^\mathrm{z}_{\sigma_k}(y_k^-, z_k^-)\| \leq \alpha^\mathrm{z}_{\sigma_k}(y_k^-, \|z_k^-\|) \quad (11)$$

Notice that due to mode changes, a jump may occur as a result of changes in the output map. Therefore, α_m must also account for this potential change in the output. Moreover, in the refinement section, we will modify this assumption—Assumption **(J2)′**—to account for asymmetry in the jump heights.

Remark 3.1. *The framework in* (1)*, together with Assumption **(S4)**, accommodates modes of different internal state dimensions. Provided the switching sequence is known and the jump maps capture the coordinate changes induced by mode-dependent internal states, the method applies without restriction. For notational simplicity, we denote the overall state dimension generically by n in* (1) *and thereafter.*

Finally, several assumptions and properties related to the desired funnel and the reference output are outlined below.

(P1) The desired funnel boundary is given by $\psi^\mathrm{d} : [t_0, \infty) \to (0, \infty)$, which is assumed to be continuous, differentiable almost everywhere, convex, bounded and with bounded derivative; furthermore, we assume it is uniformly bounded away from zero. In particular, there are constants $\underline{\psi^\mathrm{d}} > 0$ and $\overline{d\psi^\mathrm{d}} > 0$ such that

$$\psi^\mathrm{d}(t_0) \geq \psi^\mathrm{d}(t) \geq \underline{\psi^\mathrm{d}} \;\text{ and }\; 0 > \dot{\psi}^\mathrm{d}(t) > -\overline{d\psi^\mathrm{d}} \quad \forall t \geq 0.$$

(P2) The initial error, $e(t_0)$, resides within the desired funnel boundary, i.e.

$$|e(t_0)| < \psi^\mathrm{d}(t_0).$$

(P3) The reference output $y^\mathrm{r} : [t_0, \infty) \to \mathbb{R}$ is continuously differentiable, bounded, and has a bounded derivative. While $y^\mathrm{r}(t)$ is unknown a priori and available only during the experiment, its bounds are assumed to be known:

$$\underline{Y^\mathrm{r}} \leq y^\mathrm{r}(t) \leq \overline{Y^\mathrm{r}}, \quad (12)$$

where $\underline{Y^\mathrm{r}}$ and $\overline{Y^\mathrm{r}}$ denote the global bounds of $y^\mathrm{r}(t)$.

Similarly, the derivative bounds are known:

$$\underline{dY^\mathrm{r}} \leq \dot{y}^\mathrm{r}(t) \leq \overline{dY^\mathrm{r}}, \quad (13)$$

where $\underline{dY^\mathrm{r}}$ and $\overline{dY^\mathrm{r}}$ are the global bounds on $\dot{y}^\mathrm{r}(t)$.

Additionally, we define:

$$Y^\mathrm{r}_\mathrm{max} = \max\left(|\underline{Y^\mathrm{r}}|, |\overline{Y^\mathrm{r}}|\right). \quad (14)$$

Remark 3.2. *The main restrictive assumptions are: (i) each mode has relative degree one, although extensions to higher relative degree systems are conceivable but technically more involved; and (ii) the setting is SISO, though extending to MIMO systems should be feasible. The approach is not limited by the dimension of the internal state, but practical limitations arise from the number of switches, since verifying required boundedness conditions (further will be investigated) becomes difficult for nonperiodic switching with infinitely many switches.*

Table 1 provides a structured summary of the prior information available to us, the unknown quantities that remain inaccessible, and the parameters that become available only during the experiment. This clarifies that the proposed method is not entirely model-free, but is tailored for scenarios where only limited model information is available. In contrast to the classical funnel controller [14], which relies solely on output measurements and structural assumptions, our approach additionally requires certain bounds (cf. Table 1). However, aside from the earliest works, the use of such bounds has become standard in the funnel control literature (see, e.g., [32]).

Unknown	**Known a Priori**	**Known at Runtime**
f_m, g_m	$g_\mathrm{m} > 0$	-
J_m	α_m	-
f^z_m	b_m, Z_0^+	-
J^z_m	$\alpha^\mathrm{z}_\mathrm{m}$	-
-	$\psi^\mathrm{d}(t_0)$, $\underline{\psi^\mathrm{d}}$, $\overline{d\psi^\mathrm{d}}$	$\psi^\mathrm{d}(t)$
-	$[\underline{t}_k, \bar{t}_k]$, $\tau_\mathrm{s} > 0$	t_k
-	Mode sequence $(\sigma_k)_{k\in\mathbb{N}_0}$	$\sigma(t)$
-	$\underline{Y^\mathrm{r}}$, $\overline{Y^\mathrm{r}}$	$y^\mathrm{r}(t)$
-	$\underline{dY^\mathrm{r}}$, $\overline{dY^\mathrm{r}}$	$\dot{y}^\mathrm{r}(t)$

Table 1: Overview of parameter availability, categorizing parameters into those known a priori, determined during runtime, and those inaccessible.

3.2. Core Algorithm Development

In this section, we develop an adjusted funnel boundary tailored to impulsive switched systems. The overall concept is illustrated in Fig. 1.

In the figure, the variable η_k appears. To mitigate post-jump error, we introduce η_k as the level to which the adjusted funnel boundary is temporarily contracted during the interval $\tau_\mathrm{s}/2$ preceding the k-th jump. Since

$$|e_k^+| \leq |e_k^-| + |\Delta e_k| \leq |e_k^-| + \alpha_{\sigma_k}(y_k^-, \|z_k^-\|),$$

reducing the pre-jump error $|e_k^-|$ directly tightens the bound on the post-jump error $|e_k^+|$.

The constants η_k are assumed to satisfy

$$0 < \eta_k \leq \psi^\mathrm{d}(\bar{t}_k), \quad \forall k. \quad (15)$$

For later use, define

$$\eta_{\max} := \max_{k\in\mathbb{N}} \eta_k,$$

and assume that it is finite and positive.

The adjusted funnel boundary is constructed as follows: It coincides with the desired funnel outside the extended region around each jump window, i.e.,

$$t \notin [\underline{t}_k - \tfrac{\tau_s}{2},\ \bar{t}_k + \tfrac{\tau_s}{2}],$$

where $\tau_s > 0$ is the dwell time from **(J1)**.

a) Before the jump: For $t \in [\underline{t}_k - \frac{\tau_s}{2},\ \underline{t}_k]$, the adjusted boundary is a connecting curve between

$$\big(\underline{t}_k - \tfrac{\tau_s}{2},\ \psi^{\mathrm{d}}(\underline{t}_k - \tfrac{\tau_s}{2})\big) \quad \text{and} \quad (\underline{t}_k, \eta_k).$$

b) During the jump window: For $t \in [\underline{t}_k, \bar{t}_k]$, where the jump can occur at any time, the adjusted funnel consists of two parallel boundaries:

$$\psi(t) = \eta_k \quad \text{and} \quad \psi(t) = \begin{cases} \psi^{\mathrm{d}}(t), & \psi^{\mathrm{d}}(\bar{t}_k) \geq E_k, \\ E_k, & \text{otherwise.} \end{cases} \tag{16}$$

where E_k represents an upper bound for $|e(t_k^+)|$. The lower boundary remains active before the jump, while the upper boundary activates immediately afterward. The precise calculation of E_k will be provided in the upcoming Section 3.3.

c) After the Jump: For $t \in [\bar{t}_k, \bar{t}_k + \tau_s/2]$, the adjusted boundary is a curve connecting:

$$(\bar{t}_k, \psi(\bar{t}_k)) \quad \text{and} \quad \big(\bar{t}_k + \tau_s/2, \psi^{\mathrm{d}}(\bar{t}_k + \tau_s/2)\big).$$

The connecting curves in a) and c) are defined by the mapping $t \mapsto c(t, t_1, \psi_1, t_2, \psi_2)$, where $t_0 < t_1 < t_2$ and $0 < \psi_2 < \psi_1$. Each curve is constructed by scaling and shifting a differentiable, monotonically increasing template function $\rho : [0,1] \to [0,1]$ satisfying the boundary conditions $\rho(0) = 0$ and $\rho(1) = 1$. The connecting curve is then defined as

$$c(t) = \psi_1 + (\psi_2 - \psi_1) \cdot \rho\left(\frac{t - t_1}{t_2 - t_1}\right). \tag{17}$$

This definition can be extended to ensure smoothness by matching derivatives at the endpoints; one possible choice is a cubic spline which was employed in Figure 1. However, in this case, a whole family of template functions ρ must be used which are parametrized by the derivatives at 0 and 1.

Nevertheless, matching derivatives at the boundaries offers no clear advantage—at least in the relative degree one scenario considered here. In fact, when estimating the required input magnitude, the dominant factor is the maximum derivative of the connecting curve. This maximum is minimized by using a straight-line connection, which corresponds to choosing

$$c(t, t_1, \psi_1, t_2, \psi_2) = \psi_1 + (\psi_2 - \psi_1)\tfrac{t - t_1}{t_2 - t_1}. \tag{18}$$

The complete procedure for constructing the adjusted funnel boundary is outlined in Algorithm 1.

Algorithm 1: Adjusted Funnel Construction

Input : $\underline{t}_k$, $\bar{t}_k$, E_k, $\forall k \in \mathbb{N}$. τ_s, t, $\psi^{\mathrm{d}}(t)$.
Output: $\psi(t)$.
if $t \in [t_0, \underline{t}_1 - \tau_s/2)$ *or* $t \in [\bar{t}_{k-1} + \tau_s/2, \underline{t}_k - \tau_s/2)$ **then**
  $\psi(t) = \psi^{\mathrm{d}}(t)$;
else if $t \in [\underline{t}_k - \tau_s/2, \underline{t}_k)$ **then**
  $\psi(t) = \psi^{\mathrm{d}}\left(\underline{t}_k - \frac{\tau_s}{2}\right) + \big(\eta_k - \psi^{\mathrm{d}}(\underline{t}_k - \frac{\tau_s}{2})\big)\rho\left(\frac{2(t-\underline{t}_k)}{\tau_s}\right)$;
else if $t \in [\underline{t}_k, t_k)$ **then**
  $\psi(t) = \eta_k$;
else if $t \in [t_k, \bar{t}_k)$ **then**
  $\psi(t) = \begin{cases} \psi^{\mathrm{d}}(t), & \psi^{\mathrm{d}}(\bar{t}_k) \geq E_k, \\ E_k, & \text{otherwise.} \end{cases}$;
else if $t \in [\bar{t}_k, \bar{t}_k + \tau/2]$ **then**
  $\psi(t) = E_k + \big(\psi^{\mathrm{d}}(\bar{t}_k + \tau_s/2) - E_k\big)\rho(2(t - \bar{t}_k)/\tau_s)$;

3.3. Determining adjusted funnel level E_k

To compute the adjusted funnel level during jump windows, we utilize the given bounds on internal states (**S2**) and jumps (**J2**).

We start with considering the initial interval $[t_0, t_1)$. Let us define

$$\begin{aligned} Y_0^{\min} &:= \underline{Y^{\mathrm{r}}} - \psi^{\mathrm{d}}(t_0) \leq \inf_{t\in[t_0,\bar{t}_1)} (y^{\mathrm{r}}(t) - \psi(t)), \\ Y_0^{\max} &:= \overline{Y^{\mathrm{r}}} + \psi^{\mathrm{d}}(t_0) \geq \sup_{t\in[t_0,\bar{t}_1)} (y^{\mathrm{r}}(t) + \psi(t)), \\ Z_0^{\max} &:= \sup_{\|z\|\leq Z_0^+, y\in[Y_0^{\min}, Y_0^{\max}]} b_{\sigma_0}(\|z\|, |y|). \end{aligned} \tag{19}$$

Then, under the assumption that the error remains within the adjusted funnel, we have that $y(t) \in [Y_0^{\min}, Y_0^{\max}]$ and hence, by utilizing **(S2)**, $\|z(t)\| \leq Z_0^{\max}$ for all $t \in [t_0, t_1)$. To estimate a bound on the jump in the output at time $t = t_k$, $k \geq 1$, and the corresponding required size of the adjusted funnel, assume inductively that we have already found a bound $Z_{k-1}^{\max}$ such that $\|z(t)\| \leq Z_{k-1}^{\max}$ for all $t \in [t_{k-1}, t_k)$. Let

$$C_k := \max_{\substack{y\in[-\eta_k+\underline{Y^{\mathrm{r}}}, \eta_k+\overline{Y^{\mathrm{r}}}] \\ \|z\|\leq Z_{k-1}^{\max}}} \alpha_{\sigma_k}(y, \|z\|),$$

then,

$$|e_k^+ - e_k^-| = |y_k^+ - y_k^-| \leq \alpha_{\sigma_k}(y_k^-, \|z_k^-\|) \leq C_k. \tag{20}$$

Provided that $|e(t_k^-)| < \eta_k$, we have,

$$|e(t_k^+)| \leq |e(t_k^-)| + C_k < \eta_k + C_k =: E_k.$$

It now remains to estimates a bound for the internal dynamics on the interval $[t_k, t_{k+1})$, which then can be used inductively to estimate the next jump bound. For that, let first

$$Z_k^+ := \sup_{\substack{y\in[-\eta_k+\underline{Y^{\mathrm{r}}}, \eta_k+\overline{Y^{\mathrm{r}}}] \\ \|z\|\leq Z_{k-1}^{\max}}} \alpha_{\sigma_k}^{\mathrm{z}}(y, \|z\|),$$

Algorithm 2: Determination of $|e(t_k^+)|$ Upper Bound

Input : $\underline{t}_k, \bar{t}_k, \eta_k, \sigma_k, b_{\mathrm{m}}, \alpha_{\mathrm{m}}, \alpha_{\mathrm{m}}^{\mathrm{z}}$ for $k \in \mathbb{N}$, $\mathrm{m} \in \Sigma$; t_0, Z_0^+, $\underline{Y^{\mathrm{r}}}$, $\overline{Y^{\mathrm{r}}}$, $\psi^{\mathrm{d}}(t)$;

Output: E_k, $k \in \mathbb{N}$.

Initialization: **(i)**: *Compute* $y(t)$ bounds in $[t_0, \bar{t}_1)$:

$$Y_0^{\max}(*) = \overline{Y^{\mathrm{r}}} + \psi^{\mathrm{d}}(t_0),\ Y_0^{\min}(*) = \underline{Y^{\mathrm{r}}} - \psi^{\mathrm{d}}(t_0).$$

(ii): *Compute* $\|z(t_1^-)\|$ bounds:

$$Z_0^{\max}(*) = \max_{\substack{\|z\| \le Z_0^+ \\ y \in [Y_0^{\min}(*),\, Y_0^{\max}(*)]}} b_{\sigma_0}(\|z\|, |y|).$$

For $k = 1, 2, 3, \ldots$**:**

Step 1: *Calculate* $|e(t_k^+)|$ bounds:

$$C_k(Z_{k-1}^{\max,*}) = \sup_{\substack{y \in [-\eta_k + \underline{Y^{\mathrm{r}}}, \eta_k + \overline{Y^{\mathrm{r}}}] \\ \|z\| \le Z_{k-1}^{\max}}} \alpha_{\sigma_k}(y, \|z\|)$$

$$E_k(Z_{k-1}^{\max,*}) = \eta_k + C_k(Z_{k-1}^{\max,*})$$

Step 2: *Compute* $\|z(t_k^+)\|$ bounds:

$$Z_k^+(Z_{k-1}^{\max,*}) = \sup_{\substack{y \in [-\eta_k + \underline{Y^{\mathrm{r}}}, \eta_k + \overline{Y^{\mathrm{r}}}] \\ \|z\| \le Z_{k-1}^{\max}}} \alpha_{\sigma_k}^{\mathrm{z}}(y, \|z\|)$$

Step 3: *Determine* $\psi(\underline{t}_k)$:

$$\psi_{\underline{k}}(Z_{k-1}^{\max,*}) = \begin{cases} \psi^{\mathrm{d}}(\underline{t}_k), & \psi^{\mathrm{d}}(\bar{t}_k) \ge E_k(Z_{k-1}^{\max,*}), \\ E_k(Z_{k-1}^{\max,*}), & \text{otherwise.} \end{cases}$$

Step 4: *Compute* $y(t)$ bounds in $[\underline{t}_k, \bar{t}_{k+1})$:

$$Y_k^{\max}(Z_{k-1}^{\max,*}) = \overline{Y^{\mathrm{r}}} + \psi_{\underline{k}}(Z_{k-1}^{\max,*})$$
$$Y_k^{\min}(Z_{k-1}^{\max,*}) = \underline{Y^{\mathrm{r}}} - \psi_{\underline{k}}(Z_{k-1}^{\max,*}).$$

Step 5: *Compute* $\|z(t_{k+1}^-)\|$ bounds:

$$Z_k^{\max}(Z_{k-1}^{\max,*}) = \max_{\substack{\|z\| \le Z_k^+(Z_{k-1}^{\max,*}) \\ y \in [Y_k^{\min}(Z_{k-1}^{\max,*}), Y_k^{\max}(Z_{k-1}^{\max,*})]}} b_{\sigma_k}(\|z\|, |y|)$$

Note: * denotes all external variables, including η_k, $\underline{Y^{\mathrm{r}}}$, $\overline{Y^{\mathrm{r}}}$.

then invoking **(J2)** we can conclude that $|e(t_k^-)| < \eta_k$ implies $\|z(t_k^+)\| \le Z_k^+$. Similar as for the initial interval let

$$Y_k^{\min} := \underline{Y^{\mathrm{r}}} - \psi_{\underline{k}}, \quad Y_k^{\max} := \overline{Y^{\mathrm{r}}} + \psi_{\underline{k}},$$

where,

$$\psi_{\underline{k}} := \max\{E_k, \psi^{\mathrm{d}}(\underline{t}_k)\},$$

then $|e(t)| < \psi(t)$ implies $y(t) \in [Y_k^{\min}, Y_k^{\max}]$ on $[t_k, t_{k+1})$. Consequently, we can estimate the desired bound $Z_k^{\max}$ for the internal dynamics on the interval $[t_k, t_{k+1})$ by

$$Z_k^{\max} := \max_{\substack{y \in [Y_k^{\min}, Y_k^{\max}] \\ \|z\| \le Z_k^+}} b_{\sigma_k}(\|z\|, |y|). \tag{21}$$

Algorithm 2 summarizes these steps.

Remark 3.3. *In certain cases, the switching sequence may be unavailable. Nonetheless, it remains feasible to determine the adjusted funnel boundary. In these instances, instead of computing the supremum of the functions* b_{σ_k}, α_{σ_k}, *and* $\alpha_{\sigma_k}^z$ *for the specific mode* σ_k *over the given domain, we must consider the worst-case scenario by taking the maximum over all modes. Formally, we define*

$$Z_k^{\max} = \max_{\mathrm{m} \in \Sigma} \max_{\substack{y \in [Y_k^{\min}, Y_k^{\max}] \\ \|z\| \le Z_k^+}} b_{\mathrm{m}}(\|z\|, |y|),$$

$$C_k = \max_{\mathrm{m} \in \Sigma} \sup_{\substack{y \in [-\eta_k + \underline{Y^{\mathrm{r}}}, \eta_k + \overline{Y^{\mathrm{r}}}] \\ \|z\| \le Z_{k-1}^{\max}}} \alpha_{\mathrm{m}}(y, \|z\|),$$

$$Z_k^+ = \max_{\mathrm{m} \in \Sigma} \sup_{\substack{y \in [-\eta_k + \underline{Y^{\mathrm{r}}}, \eta_k + \overline{Y^{\mathrm{r}}}] \\ \|z\| \le Z_{k-1}^{\max}}} \alpha_{\mathrm{m}}^z(y, \|z\|).$$

3.4. Funnel Control with Adjusted Boundaries

In this section we employ the adjusted funnel boundary $\psi(t)$, computed in Algorithms 1–2, to design a funnel controller tailored for impulsive switched systems. The main result is stated in the following theorem, followed by further discussion.

Theorem 3.4. *Consider the system described in (1) under Assumptions* ***(S1)****–****(S3)****, with jump bounds specified by Assumption* ***(J2)****, and a reference output* $y^{\mathrm{r}}(t)$ *satisfying Assumption* ***(P3)****. Let the adjusted funnel boundary* $\psi(t)$ *be computed using Algorithms 1–2, which rely on the desired funnel* $\psi^{\mathrm{d}}(t)$ *from Assumption* ***(P1)****, the jump windows from Assumption* ***(J1)****, and the constants* η_k *defined in* (15)*. Then the classical funnel controller*

$$u(t) = -k(t)e(t),\ k(t) = \frac{1}{\psi(t) - |e(t)|},\ e(t) = y(t) - y^{\mathrm{r}}(t),$$

ensures that the tracking error satisfies

$$|e(t)| < \psi(t), \quad \forall t \in [t_0, \infty),$$

provided that the initial error satisfies

$$|e(t_0)| < \psi^{\mathrm{d}}(t_0).$$

Proof. We proceed by induction on k. For the base case on $[t_0, t_1)$, the assumption $|e(t_0)| < \psi^{\mathrm{d}}(t_0) = \psi(t_0)$ and Lemma 2.2 imply that, under the classical funnel controller with the adjusted funnel ψ, the error remains within ψ for all $t \in [t_0, t_1)$; in particular, $e(t_1^-)$ is well defined and satisfies $|e(t_1^-)| < \eta_1$. For the induction step, assume $|e(t_k^-)| < \eta_k \le \psi(t_k)$. By the construction in the previous section, the post-jump bound satisfies $|e(t_k^+)| < E_k \le \psi(t_k)$. Applying Lemma 2.2 on $[t_k, t_{k+1})$ with initial condition $|e(t_k^+)| < \psi(t_k)$ yields $|e(t)| < \psi(t)$ for all $t \in [t_k, t_{k+1})$. In particular, just before the next jump we have $|e(t_{k+1}^-)| < \eta_{k+1} \le \psi(t_{k+1})$. This completes the induction. □

Remark 3.5. *The proposed method can be extended easily to the case that the error jump is (additionally) induced by jumps in the reference signal, provided that their bounds are known. The error jump bound in* (20) *has then to be replaced by*

$$|e_k^+ - e_k^-| \leq \alpha_{\sigma_k}(y(t_k^-), z(t_k^-)) + \alpha_{\sigma_k}^{\mathrm{r}},$$

where $\alpha_{\sigma_k}^{\mathrm{r}}$ *represents the known bounds on reference signal jumps; the calculation of* C_k *can then easily be adjusted accordingly.*

Remark 3.6. *One of the primary features of the controller is that during the continuous evolution of the system, i.e., over the interval* $[t_k, t_{k+1})$*, various types of funnel controllers can be employed. This includes advanced variants that limit the derivative of the error [32] or which employ some additional machine learning methods [33].*

4. Control Input Analysis

Theorem 3.4 guarantees that the tracking error remains within the adjusted funnel $\psi(t)$, even in the presence of jumps, and that the funnel level does not blow up in finite time. However, it does not ensure boundedness as $t \to \infty$.

For example, in the introductory case with $\mu = 0.3$, applying Algorithms 1–2 (with appropriate bounds on $z(t)$ and $y(t_k^+)$) yields an adjusted funnel $\psi(t)$ that diverges. In general, as the funnel level grows without bound, the control input required to return the error to the desired funnel may also become unbounded.

To address this issue, we first provide sufficient conditions that ensure boundedness of the adjusted funnel, formalized in a theorem. Using these results, we then derive an explicit quantitative bound on the control input and conclude the section with a numerical example.

4.1. Sufficient Conditions for Bounded Control Input

As shown in Algorithm 2, the post-jump error C_k depends on the internal states bound $Z_k^{\max}$ and on external quantities (bounds of $y^{\mathrm{r}}(t)$ and η_k), which are assumed bounded; hence, boundedness of the post-jump error—and hence of the input—as $t \to \infty$ reduces to establishing boundedness of the internal state, as formalized in the following lemma.

Lemma 4.1. *The adjusted funnel computed via Algorithms 1 and 2 remains bounded if the sequence* $\{Z_k^{\max}\}_{k=0}^{\infty}$ *from Step 5 of Algorithm 2 is uniformly bounded by some* $M_z \geq 0$*, i.e.,* $Z_k^{\max} \leq M_z$ *for all* $k \in \mathbb{N}$*.*

Proof. We first show that the sequence C_k of upper bounds on $|e(t_k^+) - e(t_k^-)|$ is uniformly bounded. In fact, with

$$M_{\mathrm{c}} := \sup_{\mathrm{m}\in\Sigma} \sup_{\substack{y\in[-\eta_{\max}+\underline{Y^{\mathrm{r}}},\eta_{\max}+\overline{Y^{\mathrm{r}}}]\\ \|z\|\leq M_z}} \alpha_{\mathrm{m}}(y, \|z\|),$$

we immediately see from Step 1 of Algorithm 2 together with $Z_k^{\max} \leq M_z$, $\eta_k \leq \eta_{\max}$ and $\underline{Y^{\mathrm{r}}} \leq y^{\mathrm{r}}(t) \leq \overline{Y^{\mathrm{r}}}(t)$ that $C_k \leq M_c$. Altogether, we then have

$$\psi(t) \leq \max\{\psi^{\mathrm{d}}(t), M_c + \eta_{\max}\} \quad \forall t \geq t_0,$$

due to the monotonicity assumption of the connecting function c; boundedness of ψ now follows from the boundedness of ψ^{d}. □

In view of Lemma 4.1, we now present conditions under which the sequence $Z_k^{\max}$ remains bounded. Towards this goal, introduce the mapping $\Phi_{\mathrm{m}}^{\mathrm{B}} : \mathbb{R}_{\geq 0} \to \mathbb{R}_{\geq 0}$, as follows:

$$\Phi_{\mathrm{m}}^{\mathrm{B}}(z) := \max_{Y^{\mathrm{r}}\in[\underline{Y^{\mathrm{r}}},\overline{Y^{\mathrm{r}}}]} b_{\mathrm{m}}\Big(\alpha_{\mathrm{m}}^{z,\sup}(Y^{\mathrm{r}}, z), Y_{\max}^{\mathrm{r}} + \max\{\eta_{\max} + \alpha_{\mathrm{m}}^{\sup}(Y^{\mathrm{r}}, z), \psi^{\mathrm{d}}(t_0)\}\Big) \tag{22}$$

where,

$$\begin{aligned} \alpha_{\mathrm{m}}^{\sup}(Y^{\mathrm{r}}, z) &:= \sup_{y\in[-\eta_{\max}-Y^{\mathrm{r}},\eta_{\max}+Y^{\mathrm{r}}]} \alpha_{\mathrm{m}}(y, \|z\|),\\ \alpha_{\mathrm{m}}^{z,\sup}(Y^{\mathrm{r}}, z) &:= \sup_{y\in[-\eta_{\max}-Y^{\mathrm{r}},\eta_{\max}+Y^{\mathrm{r}}]} \alpha_{\mathrm{m}}^{\mathrm{z}}(y, \|z\|). \end{aligned} \tag{23}$$

It is easy to see that

$$Z_k^{\max} \leq \Phi_{\sigma_k}^{\mathrm{B}}(Z_{k-1}^{\max}).$$

Unlike $Z_k^{\max}(Z_{k-1}^{\max}, \eta_k, \underline{Y}^r, \overline{Y}^r)$ (Algorithm 2, Step 5), the function $\Phi_{\sigma}^{\mathrm{B}}(z)$ depends only on z. Hence, to verify the assumption of Lemma 4.1, it suffices to study the asymptotic behavior of the nonlinear discrete-time system

$$z_{k+1} = \Phi_{\sigma_{k+1}}^{\mathrm{B}}(z_k), \qquad z_0 = Z_0^{\max}. \tag{24}$$

To analyze the asymptotic behavior of (24) more precisely, it is useful to characterize structural properties of the map Φ^{B}. For this purpose, we introduce the notions of *affine-boundedness* and *affine-contractiveness*, formalized in the following definition.

Definition 4.2. *Let* $Z_1, \ldots, Z_n, W$ *be normed vector spaces. A function* $T : Z_1 \times \cdots \times Z_n \to W$ *is said to be* $(\boldsymbol{\lambda}, L)$-affine-bounded *on a subset* $D \subseteq Z_1 \times \cdots \times Z_n$ *if there exist constants* $\lambda_1, \ldots, \lambda_n \geq 0$ *and* $L \geq 0$ *such that, for all* $(z_1, \ldots, z_n) \in Z_1 \times \cdots \times Z_n$*,*

$$\|T(z_1, \ldots, z_n)\|_W \leq \sum_{i=1}^{n} \lambda_i \|z_i\|_{Z_i} + L.$$

Here, $\boldsymbol{\lambda} = (\lambda_1, \ldots, \lambda_n) \in \mathbb{R}_{\geq 0}^n$*. In the special case where* $n = 1$*, and* $T : Z_1 \to W$ *with* $Z_1 \subseteq W$*, if* $\lambda_1 < 1$*, then* T *is said to be* affine-contractive*.*

This definition characterizes maps with controlled growth. The $(\boldsymbol{\lambda}, L)$-affine-bounded condition ensures that the norm of the output of a function $T(z_1, \ldots, z_n)$ is bounded above by an affine combination of the input norms, $\|z_i\|$. The following lemma shows that this class is closed under composition.

Lemma 4.3. *Let X and $Z_1, \dots, Z_n, W$ be normed vector spaces. For each $i = 1, \dots, n$, let $\alpha_i : X \to Z_i$ be (μ_i, M_i)-affine-bounded on a subset $E_i \subseteq X$. Let $b : Z_1 \times \cdots \times Z_n \to W$ be $(\boldsymbol{\lambda}, L)$-affine-bounded on a subset $D \subseteq Z_1 \times \cdots \times Z_n$. Define the shared domain*

$$\widetilde{D} := \{z \in E_1 \cap \cdots \cap E_n \,:\, (\alpha_1(z), \dots, \alpha_n(z)) \in D\}.$$

Then the composition

$$T(z) := b\,(\alpha_1(z), \dots, \alpha_n(z))$$

defines a function $T : \widetilde{D} \to W$, and T is (λ', L')-affine-bounded on $\widetilde{D}$, where

$$\lambda' := \sum_{i=1}^{n} \lambda_i \mu_i, \qquad L' := \sum_{i=1}^{n} \lambda_i M_i + L.$$

That is, for all $z \in \widetilde{D}$,

$$\|T(z)\|_W \le \lambda' \|z\|_X + L'.$$

Proof. Let $z \in \widetilde{D}$. Then $z \in E_i$ for all i, and $(\alpha_1(z), \dots, \alpha_n(z)) \in D$. Since each α_i is affine-bounded on E_i, we have

$$\|\alpha_i(z)\|_{Z_i} \le \mu_i \|z\|_X + M_i.$$

Applying the affine bound for b, we get

$$\begin{aligned}
\|T(z)\|_W &= \|b(\alpha_1(z), \dots, \alpha_n(z))\|_W \\
&\le \sum_{i=1}^{n} \lambda_i \|\alpha_i(z)\|_{Z_i} + L \\
&\le \sum_{i=1}^{n} \lambda_i (\mu_i \|z\|_X + M_i) + L \\
&= \underbrace{\left(\sum_{i=1}^{n} \lambda_i \mu_i\right)}_{=\lambda'} \|z\|_X + \underbrace{\left(\sum_{i=1}^{n} \lambda_i M_i + L\right)}_{=L'}.
\end{aligned}$$

Therefore, T is (λ', L')-affine-bounded on $\widetilde{D}$. □

Next, we apply Lemma 4.3 to our setting and show that if $\alpha_{\mathrm{m}}^{\sup}, \alpha_{\mathrm{m}}^{\mathrm{z,sup}}$ and b_{m} are affine-bounded, then so is Φ^{B}. Fix $Y^r \in [\underline{Y}^r, \overline{Y}^r]$. Let

$$\begin{aligned}
\alpha_1(z) &= \alpha_{\mathrm{m}}^{\mathrm{z,sup}}(Y^r, z), \\
\alpha_2(z) &= Y_{\max}^r + \max\{\eta_{\max} + \alpha_{\mathrm{m}}^{\sup}(Y^r, z),\, \psi^{\mathrm{d}}(t_0)\},
\end{aligned}$$

each (μ_i, M_i)-affine-bounded on E_1, E_2. If $b_{\mathrm{m}} : Z \times Z \to Z$ is $(\lambda_1, \lambda_2; L)$-affine-bounded on D_{m}, set

$$\widetilde{D}_{\mathrm{m}} = \{z \in E_1 \cap E_2 : (\alpha_1(z), \alpha_2(z)) \in D_{\mathrm{m}}\}.$$

By Lemma 4.3,

$$\|b_{\mathrm{m}}(\alpha_1(z), \alpha_2(z))\| \le \lambda_i' \|z\| + L_i', \quad (i = 1, 2)$$

where

$$\begin{aligned}
\lambda_1' &= \lambda_1\mu_1 + \lambda_2\mu_2, & L_1' &= \lambda_1 M_1 + \lambda_2(Y_{\max}^r + \eta_{\max} + M_2) + L, \\
\lambda_2' &= \lambda_1\mu_1, & L_2' &= \lambda_1 M_1 + \lambda_2(Y_{\max}^r + \psi^{\mathrm{d}}(t_0)) + L.
\end{aligned}$$

Hence with $\lambda' = \max_i \lambda_i'$, $L' = \max_i L_i'$ one gets

$$\|b_{\mathrm{m}}(\alpha_1(z), \alpha_2(z))\| \le \lambda' \|z\| + L', \quad \forall z \in \widetilde{D}_{\mathrm{m}}.$$

Since everything is uniform in Y^r, the same λ', L' work when taking $\sup_{Y^r \in [\underline{Y}^r, \overline{Y}^r]}$. Therefore, the function $\Phi_{\mathrm{m}}^{\mathrm{B}}(z)$ is (λ', L')-affine-bounded on $\widetilde{D}_{\mathrm{m}}$.

It is important to note that Lemma 4.3 provides only a sufficient condition for affine-boundedness. In particular, there may exist cases where the functions α or α^{z} exhibit superlinear growth in z, yet their composition with b results in a function Φ^{B} that is affine-bounded.

The following theorem provides sufficient conditions for the boundedness of the adjusted funnel boundary using the $\Phi_{\mathrm{m}}^{\mathrm{B}}$ maps.

Theorem 4.4. *Consider the system described by (1), subject to Assumptions **(S1)**–**(S3)**, with jump bounds given by Assumption **(J2)**, and a reference output $y^{\mathrm{r}}(t)$ satisfying Assumption **(P3)**. Each mode* m *is associated with a map $\Phi_{\mathrm{m}}^{B} : \mathbb{R}_{\ge 0} \to \mathbb{R}_{\ge 0}$, defined in* (22)*. The classification of each mode depends on the properties of its corresponding Φ_{m}^{B} map, which is $(\lambda_{\mathrm{m}}, L_{\mathrm{m}})$-affine-bounded over*

$$\mathcal{D}_{\mathrm{m}} := \bigcup_{k:\Phi_{\sigma_{k+1}}^{\mathrm{B}} = \Phi_{\mathrm{m}}^{B}} \left\{\Phi_{\sigma_k}^{B} \circ \cdots \circ \Phi_{\sigma_2}^{B} \circ \Phi_{\sigma_1}^{B}(Z_0^{\max})\right\}, \quad (25)$$

where $Z_0^{\max}$ is defined in (19)*.*

*Let the adjusted funnel boundary $\psi(t)$ be computed using Algorithms (1) –(2), which depend on the desired funnel $\psi^{\mathrm{d}}(t)$ from Assumption **(P1)**, the jump windows from Assumption **(J1)**, and the constants η_k from* (15)*.*

A sufficient condition for the boundedness of the adjusted funnel is that there exist constants $M_\lambda \ge 0$ and $M_{\mathrm{L}} \ge 0$, independent of k*, such that for all $k \in \mathbb{N}$:*

$$\prod_{i=1}^{k} \lambda_{\sigma_i} \le M_\lambda, \quad (26)$$

$$\sum_{j=1}^{k} \left(\prod_{i=j+1}^{k} \lambda_{\sigma_i}\right) L_{\sigma_j} \le M_{\mathrm{L}}. \quad (27)$$

Under these conditions, an upper bound on the jump heights is given by:

$$M_c = \max_{\mathrm{m} \in \Sigma} \sup_{\substack{y \in [-\eta_{\max} + \underline{Y^{\mathrm{r}}}, \eta_{\max} + \overline{Y^{\mathrm{r}}}] \\ \|z\| \le M_z}} \alpha_{\mathrm{m}}(y, \|z\|), \quad (28)$$

where M_z is given by:

$$M_z = M_\lambda Z_0^{\max} + M_{\mathrm{L}}, \quad (29)$$

Proof. As shown in Lemma 4.1, the boundedness of $\{C_k\}_{k=1}^{\infty}$ ensures the boundedness of $\psi(t)$, and by the same lemma, the boundedness of $\{Z_k^{\max}\}_{k=0}^{\infty}$ implies the boundedness of $\{C_k\}_{k=1}^{\infty}$.

The set $\mathcal{D}_{\mathrm{m}}$ represents the union of all domains reached just before each occurrence of mode m, as dictated by the mode sequence σ_k, thereby covering every possible pre-m state of $\Phi_{\mathrm{m}}^{\mathrm{B}}$.

We observed that $Z_k^{\max} \leq \Phi_{\sigma_k}^{\mathrm{B}}(Z_{k-1}^{\max})$, leading to the recursive inequality:

$$Z_k^{\max} \leq \lambda_{\sigma_k} Z_{k-1}^{\max} + L_{\sigma_k}. \tag{30}$$

Expanding this recursively yields:

$$Z_k^{\max} \leq \left(\prod_{i=1}^{k} \lambda_{\sigma_i}\right) Z_0^{\max} + \sum_{j=1}^{k} \left(\prod_{i=j+1}^{k} \lambda_{\sigma_i}\right) L_{\sigma_j}, \tag{31}$$

From (31), the boundedness of the first term by M_λ (as in (26)) and the second term by M_{L} (as in (27)) ensures that $Z_k^{\max}$ remains bounded. Thus, an upper bound for $Z_k^{\max}$ is given by:

$$Z_k^{\max} \leq M_\lambda Z_0^{\max} + M_{\mathrm{L}} := M_{\mathrm{z}}, \quad \forall k \in \mathbb{N}.$$

Finally, we determine the upper bound for the jump heights by maximizing the supremum of α_{m} across all modes. The error before each jump satisfies:

$$-\eta_k + \underline{Y^{\mathrm{r}}} < y(t_k^-) < \eta_k + \overline{Y^{\mathrm{r}}},$$

which implies:

$$-\eta_{\max} + \underline{Y^{\mathrm{r}}} < y(t_k^-) < \eta_{\max} + \overline{Y^{\mathrm{r}}}, \quad \forall k \in \mathbb{N}.$$

Hence, the largest feasible input domain for all α_{m} functions is:

$$[-\eta_{\max} + \underline{Y^{\mathrm{r}}}, \eta_{\max} + \overline{Y^{\mathrm{r}}}] \times [0, M_{\mathrm{z}}].$$

Evaluating α_{m} for all $\mathrm{m} \in \Sigma$ over this domain and taking the maximum yields the bound in (28). □

Remark 4.5. *There are alternative methods to directly verifying the boundedness of the series in equation (27). One approach is to define the following sequences [34]:*

$$P_\lambda^k := \left\{ \prod_{i=j+1}^{k} \lambda_{\sigma_i} \right\}_{j=1}^{k-1}, \quad P_L^k := \{L_{\sigma_j}\}_{j=1}^{k},$$

$$P_{\lambda^2}^k := \left\{ \left(\prod_{i=j+1}^{k} \lambda_{\sigma_i} \right)^2 \right\}_{j=1}^{k-1}, \quad P_{L^2}^k := \{L_{\sigma_j}^2\}_{j=1}^{k}.$$

If any of the following conditions hold, the series in equation (27) is bounded:

a) $\sum P_L^k$ *is bounded.*

b) $\sum P_\lambda^k$ *is bounded.*

c) Both $\sum P_{\lambda^2}^k$ *and* $\sum P_{L^2}^k$ *are bounded.*

There are certain scenarios where the boundedness of the adjusted funnel can be more readily determined based on the properties of the $\Phi_{\mathrm{m}}^{\mathrm{B}}$ maps or the characteristics of the switching signal. These scenarios are outlined in the following corollary.

Corollary 4.6. *1) If all modes are affine-contractive, the adjusted funnel remains bounded regardless of the switching signal. This follows from the fact that* (26) *is bounded since all* $\lambda_i < 1$. *Furthermore,* $\sum P_\lambda^k$ *in Remark 4.5 is also bounded. Considering the largest contraction factor,* $\max_{m\in\Sigma} \lambda_m$, *instead of all individual* λ_i, *the sequence forms a geometric series with a ratio less than 1. Consequently, by Remark 4.5, the series in* (27) *remains bounded.*

2) If $L_{\mathrm{m}} = 0$, $\forall \mathrm{m} \in \Sigma$, *the mere condition of boundedness of* $\prod_{k=1}^{\infty} \lambda_k$ *is sufficient to ensure the boundedness of the adjusted funnel. In this case,* $M_{\mathrm{L}} = 0$.

3) If the switching signal becomes periodic from the kth jump, define:

$$\mathcal{P} = \{\sigma_k, \sigma_{k+1}, \ldots, \sigma_{k+T}\}$$

where T *denotes the period length, and let* $\mathcal{P}[i] := \sigma_{k+i-1}$. *If* $\prod_{i=1}^{T} \lambda_{\mathcal{P}[i]} < 1$, *then the adjusted funnel remains bounded. In this case,* M_{L} *can be computed as:*

$$M_{\mathrm{L}} = \frac{N_{\lambda L}}{1 - P_\lambda},$$

where

$$N_{\lambda L} = \max_{s\in\{1,\ldots,T-1\}} \sum_{j=1}^{s-1} \left(\prod_{i=j+1}^{s} \lambda_{\mathcal{P}[i]} \right) L_{\mathcal{P}[j]} + L_{\mathcal{P}[s]} + \sum_{j=s+1}^{T} \left(\prod_{i=j-s}^{T-1} \lambda_{\mathcal{P}[a_i]} \right) L_{\mathcal{P}[j]}.$$

$$a_i = \begin{cases} s - i + 1, & i \leq s, \\ T - (i - s - 1), & i > s. \end{cases}$$

and

$$P_\lambda = \prod_{i=1}^{T} \lambda_{\mathcal{P}[i]}.$$

which holds for $t > t_k^+$.

4) Consider the special case of a system with two modes, labeled as m_1 *and* m_2. *If* $\lambda_1\lambda_2 < 1$, *then the adjusted funnel is bounded. In this case,* M_{L} *is given by:*

$$M_{\mathrm{L}} = \max\left(\frac{L_1 + \lambda_1 L_2}{1 - \lambda_1\lambda_2}, \frac{L_2 + \lambda_2 L_1}{1 - \lambda_1\lambda_2} \right)$$

Remark 4.7. *For a single-mode system with a (λ, L)-affine-contractive Φ^B, the adjusted funnel remains bounded. In this case, $\prod_{i=1}^{k} \lambda_{\sigma_i} = \lambda^k < 1$, implying $M_\lambda = 1$. The constant M_{L} can be calculated as:*

$$M_{\mathrm{L}} = \sum_{j=1}^{k} \lambda^{k-j} L = \frac{L}{1-\lambda}.$$

Consequently, M_z simplifies to:

$$M_z = Z_0^{\max} + \frac{L}{1-\lambda}.$$

Remark 4.8. *Even if the internal state dynamics are not stable, as long as the Φ^B maps are either affine-bounded or affine-contractive and the conditions of Theorem 4.4 are satisfied, we can still conclude that the adjusted funnel remains bounded over time. In fact, in such cases, the jumps in the internal states and/or output may actually help prevent the internal states from growing unbounded.*

Remark 4.9. *Consider the class of dynamical systems described by* (1)*, whose state trajectories $(y(t), z(t))$ satisfy the inequalities* (9a), (10a)*, and* (11)*. Given the jump windows $\mathcal{I}_k$ for all $k \in \mathbb{N}$ and the initial set Z_0, if the conditions of Theorem 4.4 are satisfied, then the adjusted funnel boundary $\psi(t)$, computed by Algorithms 1–2, remains invariant under the system dynamics. In other words, $\psi(t)$ is independent of any particular realization within the admissible class of systems.*

4.2. Quantitative Bounds on the Control Input

Having established the sufficient conditions for maintaining a bounded adjusted funnel, we now focus on determining a bound on the control input required to restore the error to the desired funnel.

To derive a quantitative bound for the control input, we require bounds on f_{m} and g_{m}. We assume that for each $\mathrm{m} \in \Sigma$ there exist known functions $\underline{f}_{\mathrm{m}}$, $\overline{f}_{\mathrm{m}}$, $\underline{g}_{\mathrm{m}}$ (with $\underline{g}_{\mathrm{m}} > 0$) such that, for all admissible (y, z),

$$\begin{aligned} &\underline{f}_{\mathrm{m}}(y, \|z\|) \le f_{\mathrm{m}}(y, z) \le \overline{f}_{\mathrm{m}}(y, \|z\|), \\ 0 \;<\; &\underline{g}_{\mathrm{m}}(y, \|z\|) \le g_{\mathrm{m}}(y, z). \end{aligned} \tag{32}$$

where $\underline{f}_{\mathrm{m}}, \overline{f}_{\mathrm{m}}$, and $\underline{g}_{\mathrm{m}}$ are assumed to be continuous functions, which may not necessarily represent the tightest possible bounds for f_{m} and g_{m}.

If no information is available about these bounds, then as long as the conditions of Theorem 4.4 are satisfied, we can still conclude whether the adjusted funnel remains bounded. However, it is not possible to derive a quantitative upper bound for the control input.

Proposition 4.10. *Assume the hypotheses of Theorem 4.4 and the bounds* (32) *on f_{m} and g_{m}. Let the adjusted funnel boundary $\psi(t)$ be constructed by Algorithms 1–2. Then the feedback input remains uniformly bounded:*

$$|u(t)| \le U^{\max}, \qquad \forall\, t \ge t_0,$$

where $U^{\max} := \max\left\{|u^{\min}|,\ |u^{\max}|\right\}$, with

$$u^{\min} := \frac{\underline{\theta} - F^{\max} + \underline{dY^{\mathrm{r}}}}{G^{\min}}, \quad u^{\max} := \frac{\overline{\theta} - F^{\min} + \overline{dY^{\mathrm{r}}}}{G^{\min}}. \tag{33}$$

The constants $F^{\min}$, $F^{\max}$, and $G^{\min}$ are defined by:

$$\begin{aligned} F^{\min} &= \min_{\mathrm{m}\in\Sigma} \min_{\substack{\|z\|\le M_{\mathrm{z}} \\ y\in[-E^{\max}+\underline{Y^{\mathrm{r}}},\, E^{\max}+\overline{Y^{\mathrm{r}}}]}} \underline{f}_{\mathrm{m}}(y, z), \\ F^{\max} &= \max_{\mathrm{m}\in\Sigma} \max_{\substack{\|z\|\le M_{\mathrm{z}} \\ y\in[-E^{\max}+\underline{Y^{\mathrm{r}}},\, E^{\max}+\overline{Y^{\mathrm{r}}}]}} \overline{f}_{\mathrm{m}}(y, z), \\ G^{\min} &= \min_{\mathrm{m}\in\Sigma} \min_{\substack{\|z\|\le M_{\mathrm{z}} \\ y\in[-E^{\max}+\underline{Y^{\mathrm{r}}},\, E^{\max}+\overline{Y^{\mathrm{r}}}]}} \underline{g}_{\mathrm{m}}(y, z). \end{aligned} \tag{34}$$

Here, M_{z} is given by (29)*, and $E^{\max} := \max\left\{\eta_{\max} + M_c,\, \psi^{\mathrm{d}}(0)\right\}$, with M_c defined in* (28)*. The reference bounds $\underline{dY^{\mathrm{r}}}$, $\overline{dY^{\mathrm{r}}}$ are from* (13)*.*

Also, the slope bounds $\overline{\theta}$, $\underline{\theta}$ are defined as:

$$\underline{\theta} = \min\left\{M_{\mathrm{cf}},\ -\overline{d\psi^{\mathrm{d}}}\right\}, \qquad \overline{\theta} = -\underline{\theta}, \tag{35}$$

where

$$M_{\mathrm{cf}} := \inf_{k} \inf_{t\in[0,\,\tau_{\mathrm{s}}/2]} \dot{c}_k(t),$$

with c_k denoting the connecting function from (17)*, defined on the interval $[\overline{t}_k,\, \overline{t}_k + \tau_{\mathrm{s}}/2]$. Moreover, $\overline{d\psi^{\mathrm{d}}}$ is as specified in Assumption **(P1)**.*

Proof. From the system dynamics, the output evolves as

$$\dot{y} = f_{\sigma(t)}(y, z) + g_{\sigma(t)}(y, z)u.$$

For the tracking error $e := y - y^{\mathrm{r}}$, we have

$$\dot{e} = f_{\sigma(t)}(y, z) + g_{\sigma(t)}(y, z)u - \dot{y}^{\mathrm{r}}.$$

Since $\underline{f}_{\mathrm{m}}$, $\overline{f}_{\mathrm{m}}$ and $\underline{g}_{\mathrm{m}}$ are continuous and the domain

$$[-E^{\max} + \underline{Y^{\mathrm{r}}},\, E^{\max} + \overline{Y^{\mathrm{r}}}] \times \{z : \|z\| \le M_z\}$$

is compact, the extrema in (34) are well-defined. Therefore,

$$\dot{e} \le F^{\max} + G^{\min}u - \underline{dY^{\mathrm{r}}}, \qquad \dot{e} \ge F^{\min} + G^{\min}u - \overline{dY^{\mathrm{r}}}.$$

To ensure the error remains within the funnel during recovery, Lemma 2.2 requires $\underline{\theta} \le \dot{e} \le \overline{\theta}$ over every window $[\overline{t}_k, \overline{t}_k + \tau_{\mathrm{s}}/2]$.

As stated in (35), $\underline{\theta}$—defined as the smaller of the desired funnel's initial derivative and the minimum slope of all connector functions—represents the lower bound of $\dot{\psi}(t)$. Since the error must remain between $\underline{\theta}$ and $\overline{\theta}$, we substitute (35) into the inequality bounds on $\dot{e}$ to obtain the expressions for $u^{\min}$ and $u^{\max}$ in (33). Taking the larger of their absolute values then gives the global input bound $U^{\max}$. □

Remark 4.11. *There is a strong interrelation between the dwell time τ_s and the input bound $U^{\max}$. In fact, given $U^{\max}$, the bounds*

$$\underline{\theta} = U^{\max}G^{\min} + F^{\max} - \underline{dY^{\mathrm{r}}}, \quad \overline{\theta} = U^{\max}G^{\min} + F^{\min} - \overline{dY^{\mathrm{r}}}$$

yield the admissible slope

$$\theta_{\mathrm{adm}} := \max\big(|\overline{\theta}|, |\underline{\theta}|, \overline{d\psi^d}\big).$$

For the chosen template ρ in (17), the connecting functions satisfy

$$\dot{c}_k(t) = \frac{2\big(\psi^{\mathrm{d}}(t_k + \frac{\tau_s}{2}) - E_k\big)}{\tau_s}\dot{\rho}(\cdot) \;\geq\; \frac{2(\underline{\psi^{\mathrm{d}}} - E^{\max})}{\tau_s} M_\rho,$$

with

$$M_\rho := \sup_k \max_{t\in[0,1]} \dot{\rho}_k(t),$$

which exists since $\rho \in C^1([0,1])$. Equating θ_{adm} with this lower bound yields

$$\tau_s = \frac{2(\underline{\psi^{\mathrm{d}}} - E^{\max})M_\rho}{\theta_{\mathrm{adm}}}.$$

If τ_s is given, we can reverse the above analysis to obtain a sufficient bound for $U_{\max}$.

4.3. Numerical Example: BIBO Internal States

Example 1. Consider the following academic impulsive switched system with two modes: Mode 1 has dimension $n_1 = 2$, and Mode 2 has dimension $n_2 = 3$ (see Remark 3.1).

Mode 1

$$\begin{aligned}
\dot{y}(t) &= 2z(t)y(t) - 0.2y(t) + 0.6u(t), && t \neq t_k,\\
y(t_k^+) &= 1.3y(t_k^-) + 1.4\|z(t_k^-)\|, && t = t_k,\\
\dot{z}(t) &= -2z(t) + \sqrt{|y(t)|}, && t \neq t_k,\\
z(t_k^+) &= z_2(t_k^-)/(1 + |z_2(t_k^-)|), && t = t_k.
\end{aligned}$$

Mode 2

$$\begin{aligned}
\dot{y}(t) &= z_1(t) + y(t) + u(t), && t \neq t_k,\\
y(t_k^+) &= 0.6y(t_k^-)|z(t_k^-)| + y(t_k^-), && t = t_k,\\
\dot{z}_1(t) &= -2z_1(t) + 2z_2(t), && t \neq t_k,\\
\dot{z}_2(t) &= -2z_1(t) - 2z_2(t) + \sqrt[3]{y(t)}, && t \neq t_k,\\
z_1(t_k^+) &= z(t_k^-), && t = t_k,\\
z_2(t_k^+) &= 2z(t_k^-), && t = t_k.
\end{aligned}$$

The initial conditions are $y(0) = 0.9$ and $z(0) = [0.1, 0.8]^T$. The following are the corresponding bounds for each mode.

Mode 1

$$\begin{aligned}
&b_1 = \|z(t_k^+)\| + 0.5\|y_{[t_k,t_{k+1})}\|_\infty^{\frac{1}{2}},\\
&\alpha_1 = 0.3|y(t_k^-)| + 1.4\|z(t_k^-)\|, \;\; \alpha_1^{\mathrm{z}} = 1,\\
&\overline{f}_1 = -\underline{f}_1 = 2|z(t)||y(t)| + 0.2|y(t)|, \;\; \underline{g}_1 = 0.4.
\end{aligned} \tag{36}$$

Mode 2

$$\begin{aligned}
&b_2 = \|z(t_k^+)\| + 0.5\|y_{[t_k,t_{k+1})}\|_\infty^{\frac{1}{3}},\\
&\alpha_2 = 0.6|y(t_k^-)|\|z(t_k^-)\|, \;\; \alpha_2^{\mathrm{z}} = 2.25\|z(t_k^-)\|,\\
&\overline{f}_2 = -\underline{f}_2 = \|z(t)\| + |y(t)|, \;\; \underline{g}_2 = 1.
\end{aligned} \tag{37}$$

Also, $\|z(0)\|$ is initially within the range $[0.75, 0.85]$. The system begins in Mode 2 at $t_0 = 0$, following a repeating mode sequence of $\{2, 1, 2, 1, \dots\}$ in subsequent intervals. The onset of the jump intervals occurs every five seconds, with their lengths and exact jump instance determined randomly.

The desired funnel is defined as $\psi^{\mathrm{d}}(t) = e^{-0.05t} + 0.1$ and $y^{\mathrm{r}}(t) = 0.5 + 0.5\sin(t)$. Additionally, $\eta(t_k) = \frac{1}{2}\psi^{\mathrm{d}}(\bar{t}_k)$ and $\tau_s = 1$.

To proceed, we compute Φ^{B} for both modes. Utilizing equation (22), we derive the following expressions, given that $\eta_{\max} = \eta_1 = \frac{1}{2}\psi^{\mathrm{d}}(\bar{t}_1) = 0.42$, $\underline{Y^{\mathrm{r}}} = 0, \overline{Y^{\mathrm{r}}} = 1$, and $Y^{\mathrm{r}}_{\max} = 1$.

$$\begin{aligned}
\Phi_1^B(z) &= 1 + 0.5\left(\max\{1.3\eta_{\max} + 0.3\overline{Y^{\mathrm{r}}} + 1.4z, 1.1\} + Y^{\mathrm{r}}_{\max}\right)^{\frac{1}{2}},\\
&\leq 1 + 0.5\left(\frac{1}{2}\max\{1.3 \times 0.42 + 0.3 + 1.4z, 1.1\} + 1\right),\\
&\leq 0.35z + 1.78.
\end{aligned}$$

Hence, $\Phi_1^B(z)$ is affine-contractive. To demonstrate this, we compute the upper bound on $\|z(t)\|$ assuming only Mode 1 is active, following Algorithm 2. The resulting values are illustrated in Fig. 4a. For mode 2, we have,

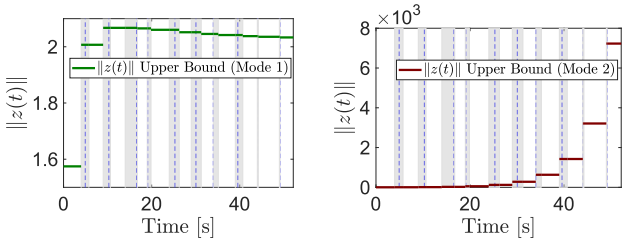

(a) Only Mode 1. (b) Only Mode 2.

Figure 4: $\|z(t)\|$ upper bound in the system of Example 1 for one mode scenarios.

$$\begin{aligned}
\Phi_2^{\mathrm{B}}(z) &= 2.25z + 0.5\left(\max\{\eta_{\max} + 0.6(\eta_{\max} + \overline{Y^{\mathrm{r}}})z, 1.1\} + Y^{\mathrm{r}}_{\max}\right)^{\frac{1}{3}},\\
&\leq 2.25z + 0.5\left(\frac{1}{3}\max\{0.42 + 0.6(0.42 + 1)z, 1.1\} + 1\right),\\
&\leq 2.39z + 0.68.
\end{aligned}$$

Therefore, mode 2 is affine-bounded but not contractive. In Fig. 4b, the $Z_k^{\max}$ sequence is depicted for the case where only Mode 2 is active.

The multi-mode system incorporating modes 1 and 2 is characterized by a joint parameter $M_\lambda = \lambda_1\lambda_2 = 0.35 \times 2.39 = 0.84 < 1$. According to Corollary 4.6, the system guarantees a bounded $Z_k^{\max}$, ensuring a bounded jump sequence, and adjusted funnel.

The procedure for computing E_k is given in Equation (38). Figures 5 and 6 illustrate the upper bound on

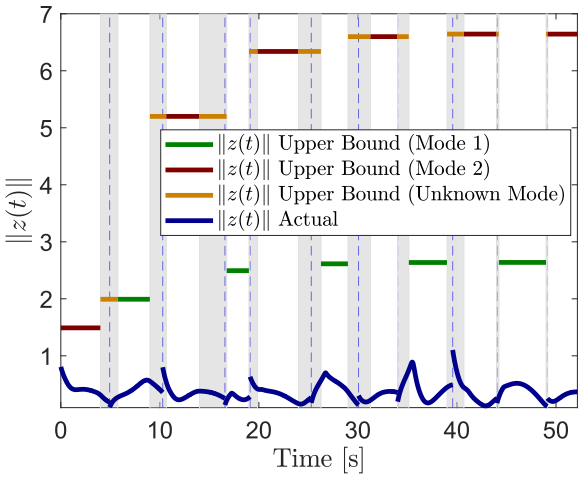

Figure 5: Evolution of $\|z(t)\|$ and its upper bound in Example 1 with both modes active.

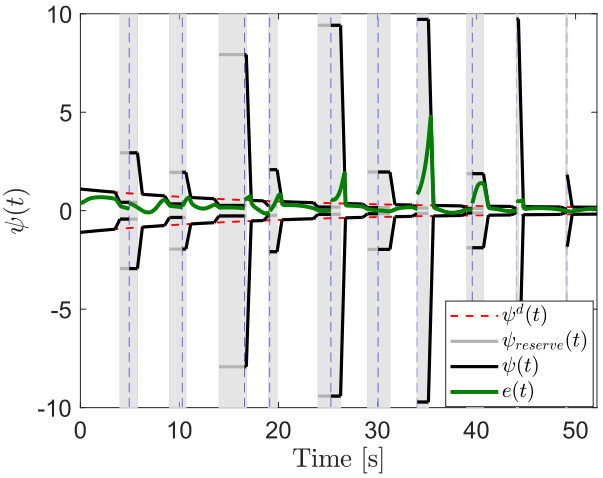

Figure 6: Computed adjusted funnel boundary and the actual error development for Example 1.

$\|z(t)\|$, along with the adjusted funnel boundary and the evolution of the error within it.

Initial conditions: $Z_0^+ = 0.85$. **Initialization:**

$$Y_0^{\max} = 1 + 1.1 = 2.1,\ Y_0^{\min} = 0 - 1.1 = -1.1$$
$$Z_0^{\max} = 0.85 + 0.5(\max(|2.1|, |-1.1|))^{\frac{1}{3}} = 1.49.$$

For $k = 1, 2, 3, \ldots$:

$$C_k = \begin{cases} 0.3(\eta_k + 1) + 1.4 Z_{k-1}^{\max} & \sigma_k = 1, \\ 0.6(\eta_k + 1) Z_{k-1}^{\max} & \sigma_k = 2, \end{cases}, \quad E_k = \eta_k + C_k, \tag{38}$$

$$Z_k^+ = \begin{cases} 1 & \sigma_k = 1, \\ 2.25 Z_{k-1}^{\max} & \sigma_k = 2, \end{cases}, \underline{\psi_k} = \begin{cases} E_k, & e^{-0.05\underline{t}_k} + 0.1 < E_k, \\ e^{-0.05\underline{t}_k} + 0.1, & \text{otherwise}, \end{cases}$$

$$Y_k^{\max} = 1 + \underline{\psi_k}; Y_k^{\min} = -\underline{\psi_k},$$

$$Z_k^{\max} = \begin{cases} Z_k^+ + 0.5(\max(|Y_k^{\min}|, |Y_k^{\max}|))^{\frac{1}{2}} & \sigma_k = 1, \\ Z_k^+ + 0.5(\max(|Y_k^{\min}|, |Y_k^{\max}|))^{\frac{1}{3}} & \sigma_k = 2, \end{cases}$$

To determine an upper bound on the jump height in accordance with (28), the value of M_z must first be computed. Given the parameters $L_1 = 1.78$, $L_2 = 0.68$, $\lambda_1 = 0.35$, and $\lambda_2 = 2.39$, and noting that mode 2 occurs first, corollary 4.6 (item 4) implies that $M_L = 12.34$. Furthermore, with $Z_0 = Z_0^{\max} = 1.49$ and $M_\lambda = 0.84$, we find $M_z = 13.59$.

To compute an upper bound on the output jump, the maximum values of α_m for both modes must be evaluated. Using (28), the computations are as follows:

$$\max(\alpha_1) = \max_{-0.42 \le y \le 1.42,\ \|z\| \le 13.59} (0.3|y(t)| + 1.4\|z(t)\|) = 19.45,$$
$$\max(\alpha_2) = \max_{-0.42 \le y \le 1.42,\ \|z\| \le 13.59} (0.6|y(t)|\|z(t)\|) = 11.58. \tag{39}$$

Thus, $M_c = 19.45$, and an upper bound on the error is determined as $E^{\max} = \eta_{\max} + M_c = 0.42 + 19.45 = 19.87$.

Given $\underline{\psi}^d = 0.1$, $E^{\max} = 19.87$, and $\tau_s = 1$, the maximum derivative of the linear connecting functions is $\overline{\theta} = 2(\underline{\psi}^d - E^{\max})/\tau_s = -39.54$. With $M_z = 13.59$, $\overline{dY^r} = -\overline{dY^r} = 0.5$, $F^{\max} = -F^{\min} = 571$, and $G^{\min} = 0.4$, it follows that $U^{\max} = 1331$.

As shown in Figures. 5 and 6, whenever $\|z(t_k^-)\|$ upper bound is large—such as after the second or fourth jump—the upper bound on $|e_k^+|$ increases. Conversely, when $\|z(t_k^-)\|$ upper bound is relatively small—such as after the third or fifth jump—the adjusted funnel level is also low. This is because both α maps depend on the internal states, and variations in $\|z(t_k^-)\|$ upper bound directly influence the error jump bounds.

One might argue that the α maps also depend on e_k^-. However, the key distinction is that e_k^- can be regulated by shrinking the adjusted funnel before each jump. In contrast, $\|z(t_k^-)\|$ is not directly controllable and plays a dominant role in determining the jump height bounds.

Part II: Refinements and Extensions

Building on the adjusted funnel construction and boundedness guarantees for relative-degree-one impulsive switched systems, this part develops refinements that further tighten the funnel boundary and reduce the control-input bound. First, we replace the BIBO assumption with practical ISS, which, by exploiting time-dependent bounds on the internal state, yields a substantial reduction of the control-input bound and enables the design of admissible impulse-time sequences ensuring bounded inputs. In addition, we introduce algorithmic enhancements such as asymmetric jump maps, level-set refinements, and real-time boundary adaptations, all of which lead to tighter funnel boundaries. Their effectiveness is demonstrated through numerical examples.

5. Practical Input-to-State Stability of Internal States

Figure 6 shows that, although the error remains within the adjusted funnel, the funnel itself expands unnecessarily. This arises because, under the assumption of merely BIBO-stable internal dynamics, no decay of the upper bound on $\|z(t)\|$ is captured, leading to overly conservative results.

To address this, we refine the stability assumption from BIBO to ISS and update the computation of $Z^{\max}$ accordingly. In this setting, we introduce the Φ^I map, tailored to ISS dynamics, as a replacement for Φ^B. We then compare the BIBO and ISS cases in a numerical example, extend the calculation of $Z^{\max}$ by adding an intermediate refinement step to further tighten the funnel boundary, and illustrate the improvement with another example. The section concludes with the design of impulse-time sequences that guarantee boundedness of the adjusted funnel boundary.

5.1. ISS-Based Adjusted Funnel Design

As demonstrated in Example 1, the upper bound of the internal states plays a critical role in determining the adjusted funnel boundary level. Specifically, tighter bounds on $\|z(t)\|$ lead to more accurate estimates of post-jump error bounds.

In the following section, we aim to establish less conservative bounds by refining the BIBO stability assumptions on internal states. The core limitation of the BIBO property is that it provides only limited information about internal state behavior. If more insights—particularly the time evolution of $\|z(t)\|$—were available, we could more accurately track their behavior over time.

To address this, we introduce a Practical ISS version of Assumption **(S2)**, as follows:

(S2)′ For every $\mathrm{m} \in \Sigma$ and for all $t_k \le s < t < t_{k+1}$, the following holds:

$$\|z(t)\| \le \beta_{\mathrm{m}}(\|z(s^+)\|, t-s) + \gamma_{\mathrm{m}}(\|y_{[s,t)}\|_\infty) + c_{\mathrm{m}}, \quad (9b)$$

where $\beta_{\mathrm{m}} : \mathbb{R}_{\ge 0} \times \mathbb{R}_{\ge 0} \to \mathbb{R}_{\ge 0}$ and $\gamma_{\mathrm{m}} : \mathbb{R}_{\ge 0} \to \mathbb{R}_{\ge 0}$ are known $\mathcal{KL}$ and $\mathcal{K}$ continuous functions [3], respectively.

The constant $c_{\mathrm{m}} \in \mathbb{R}_{\ge 0}$ accounts for the fact that, in the absence of input, the internal states are not necessarily required to decay to zero as $t \to \infty$; it is sufficient for them to remain bounded.

The dependence of β_{m} on t allows us to account for the diminishing influence of the initial condition $\|z(s^+)\|$ over time. Assuming the internal states are Practical ISS, it is possible to find an upper bound for $\|z(t_{k+1}^-)\|$ as follows:

$$\begin{aligned}\|z(t_{k+1}^-)\| \le Z_k^{\max} &= \beta_{\sigma_k}(Z_k^+, \underline{t}_{k+1} - \bar{t}_k) \\ &+ \gamma_{\sigma_k}\left(\max_{y \in \{Y_k^{\min}, Y_k^{\max}\}} |y|\right) + c_{\sigma_k}.\end{aligned} \quad (40)$$

[3] A function $\alpha : [0,\infty) \to [0,\infty)$ is of class $\mathcal{K}$ if it is continuous, strictly increasing, and $\alpha(0) = 0$. A function $\beta : [0,\infty)^2 \to [0,\infty)$ is of class $\mathcal{KL}$ if $\beta(\cdot, t) \in \mathcal{K}$ for each fixed t, and $\beta(s,\cdot)$ is decreasing with $\beta(s,t) \to 0$ as $t \to \infty$.

Here, Z_k^+ and $Y_k^{\min\,/\,\max}$ are defined as in Algorithm 2.

Note that, unlike in (21), β belongs to the class $\mathcal{KL}$-functions and γ belongs to the class $\mathcal{K}$-functions. Therefore:

$$\sup_{r \in D, \delta t \in \Delta T} \beta(r, \delta t) = \beta\big(\sup D, \inf \Delta T\big),$$
$$\sup_{r \in D'} \gamma(r) = \gamma\big(\sup D'\big).$$

where $D = [0, Z_k^+]$, $\Delta T = \big\{t_{k+1} - t_k : t_{k+1} \in [\underline{t}_{k+1}, \bar{t}_{k+1}], t_k \in [\underline{t}_k, \bar{t}_k]\big\}$, and $D' = \max\big(|Y_k^{\min}|, |Y_k^{\max}|\big)$. Then:

$$\begin{aligned}&\sup D = Z_k^+, \quad \sup D' = \max\big(|Y_k^{\min}|, |Y_k^{\max}|\big), \\ &\inf \Delta T = \underline{t}_{k+1} - \bar{t}_k.\end{aligned}$$

simplifying the calculation of $Z_k^{\max}$. Also, we introduce the map $\Phi^{\mathrm{I}} : \mathbb{R}_{\ge 0} \times \mathbb{R}_{\ge 0} \to \mathbb{R}_{\ge 0}$,

$$\begin{aligned}\Phi_{\mathrm{m}}^{\mathrm{I}}(z, \Delta t) &= \beta_{\mathrm{m}}\big(\alpha_{\mathrm{m}}^{z,\sup}(Y_{\max}^{\mathrm{r}}, z), \Delta t\big) + \\ &\gamma_{\mathrm{m}}\big(\max\{\eta_{\max} + \alpha_{\mathrm{m}}^{\sup}(Y_{\max}^{\mathrm{r}}, z), \psi^{\mathrm{d}}(t_0)\} + Y_{\max}^{\mathrm{r}}\big) + c_{\mathrm{m}}.\end{aligned} \quad (41)$$

It follows that $Z_k^{\max} \le \Phi_{\sigma_k}^{\mathrm{I}}(Z_{k-1}^{\max}, \Delta t)$ as long as $\Delta t \le \underline{t}_k - \bar{t}_{k-1}$ for all k.

Under this construction, Theorem 4.4 remains valid. Suppose each mode m persists for at least $\tau_{\mathrm{s}} + \tau_{\mathrm{m}}$, where τ_{s} is constant across all modes and $\tau_{\mathrm{m}} \ge 0$ is mode-specific. For each mode we define the time-independent map

$$\Phi_{\mathrm{m}}^{\mathrm{I}}(z) := \Phi_{\mathrm{m}}^{\mathrm{I}}(z;\, \Delta t = \tau_{\mathrm{s}} + \tau_{\mathrm{m}}). \quad (42)$$

If the maps $\Phi_{\mathrm{m}}^{\mathrm{I}}(z)$ are either $(\lambda_{\mathrm{m}}, L_{\mathrm{m}})$-affine-bounded or affine-contractive for all $\mathrm{m} \in \Sigma$, then Theorem 4.4 ensures boundedness of the adjusted funnel boundary

In the following, we examine the effect of replacing BIBO with ISS internal dynamics in the numerical example of Section 4.3 (Example 1).

5.2. Numerical Example: ISS Internal States

In cases where we have access to the following tighter bounds, the conservative bounds in (36) and (37) in Example 1 can be replaced with:

$$\begin{aligned}&\|z(t)\| \le \|z(t_k^+)\| e^{-2t} + 0.5\|y(t)\|_\infty^{1/2}, \quad t \in [t_k, t_{k+1}), \\ &\|z(t)\| \le \|z(t_k^+)\| e^{-2t} + 0.5\|y(t)\|_\infty^{1/3}, \quad t \in [t_k, t_{k+1}).\end{aligned}$$

To calculate $\Phi_{\mathrm{m}}^{\mathrm{I}}$ maps for modes 1 and 2, we follow the procedure outlined in (41), given that $\tau_1 = 1$, $\tau_2 = 1.5$, and $\tau_{\mathrm{s}} = 1$,

$$\begin{aligned}\Phi_1^I(z, 2) &= e^{-2\times 2} + \\ &0.5\left(\max\{1.3\eta_{\max} + 0.3Y_{\max}^{\mathrm{r}} + 1.4z, 1.1\} + Y_{\max}^{\mathrm{r}}\right)^{\frac{1}{2}}, \\ &\le 0.35z + 0.79. \\ \Phi_2^{\mathrm{I}}(z, 2.5) &= 2.25e^{-2\times 2.5}z + \\ &0.5\left(\max\{\eta_{\max} + 0.6(\eta_{\max} + Y_{\max}^{\mathrm{r}})z, 1.1\} + Y_{\max}^{\mathrm{r}}\right)^{\frac{1}{3}}, \\ &\le 0.16z + 0.68.\end{aligned}$$

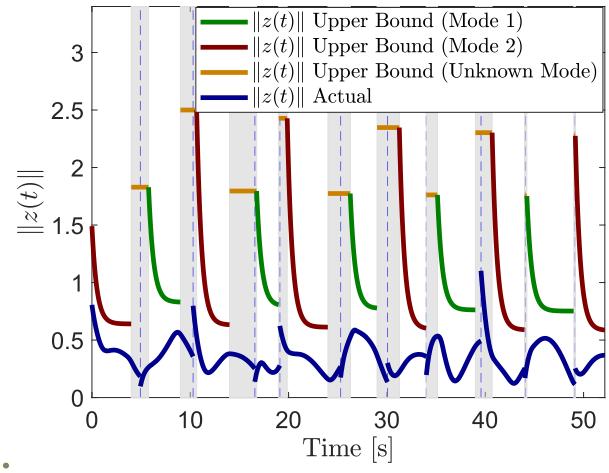

Figure 7: Development of $\|z(t)\|$ and its upper bounds for Example 1, with ISS internal dynamics.

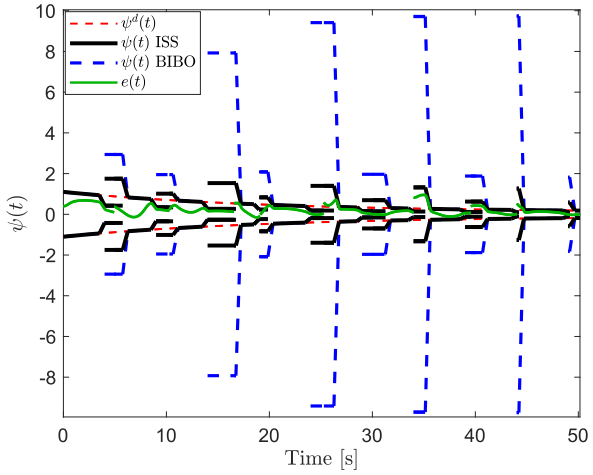

Figure 8: Adjusted funnel boundary and actual error development for Example 1, comparing the obtained $\psi(t)$ under ISS internal dynamics (solid black lines) and BIBO internal dynamics (dashed blue lines).

According to corollary 4.6 (item 1), since both Φ^{I} maps are affine-contractive, the adjusted funnel remain bounded. In this case, given $L_1 = 0.79$, $L_2 = 0.68$, $\lambda_1 = 0.35$, and $\lambda_2 = 0.16$, it follows that, $M_{\mathrm{L}} = 1.09$, and $Z_0 = Z_0^{\max} = 0.85e^{-2\times 2.5} + 0.5(\psi^{\mathrm{d}}(0)+1)^{\frac{1}{3}} = 0.65$, and therefore, $M_{\mathrm{z}} = 1.13$. Notice that, in the ISS case, M_{z} represents the upper bound of $\|z(\underline{t}_k)\|$ for all k (the worst-case scenario, namely $t_{k-1} = \bar{t}_{k-1}$ and $t_k = \underline{t}_k$).

To compute the error bounds, similar to (39) but with $M_{\mathrm{z}} = 1.13$, we have $\max \alpha_1 = 2.00$ and $\max \alpha_2 = 0.96$. Thus, $M_{\mathrm{c}} = 2.00$, and therefore, $E^{\max} = 2.42$.

To compute E_k, Equations (38) must be followed. However, the first term in $Z_k^{\max}$ relation should be replaced by $e^{(\underline{t}_{k+1}-\bar{t}_k)}Z_k^+$.

The $\|z(t)\|$ upper bound and the adjusted funnel boundary in this case are illustrated in Figures 7 and 8.

A notable improvement in the adjusted funnel can be observed when $z(t)$ exhibits ISS stability instead of BIBO stability. As depicted in Fig. 8, the maximum adjusted funnel level—equivalently, the maximum permissible error—reaches 9.74 in the BIBO-stable case, whereas in the ISS-stable case, this value is reduced to 1.75. Moreover, the upper bound on the control input in the ISS-stable case is $U^{\max} = 11$, compared to $U^{\max} = 1331$ in the BIBO-stable case.

5.3. Resetting the Calculation of $Z_k^{\max}$

In previous sections, we derived the bounds $\|z(t)\|$ for all $t \in [\underline{t}_k, \bar{t}_{k+1})$ by considering the infinity norm of y over this interval. However, if y undergoes a large jump during $[\underline{t}_k, \bar{t}_k]$, the infinity norm of the output over the entire interval $[\underline{t}_k, \bar{t}_{k+1})$ will be dominated by this large value, without accounting for any subsequent decreases in y. This approach does not fully capture the expected behavior, as y typically decreases when the error returns to the desired funnel at $\bar{t}_k + \tau_{\mathrm{s}}/2$.

To address this, one approach is to compute $Z_k^{\max}$ in two steps: first, when the error upper bound is outside the desired funnel, and second, when it returns to the desired funnel. Specifically, we define:

$$\begin{aligned} Z_k^{\max,\mathrm{int}} &:= \beta_{\sigma_k}(Z_k^+, \tau_{\mathrm{s}}/2) + \\ &\quad \gamma_{\sigma_k}\left(\max_{y\in\{Y_k^{\min,\mathrm{int}}, Y_k^{\max,\mathrm{int}}\}} |y|\right) + c_{\sigma_k}, \\ Z_k^{\max} &= \beta_{\sigma_k}(Z_k^{\max,\mathrm{int}}, \underline{t}_{k+1} - (\bar{t}_k + \tau_{\mathrm{s}}/2)) + \\ &\quad \gamma_{\sigma_k}\left(\max_{y\in\{Y_k^{\min}, Y_k^{\max}\}} |y|\right) + c_{\sigma_k}. \end{aligned} \tag{43}$$

Z_k^+ is defined as before (Step 2, Algorithm 2). However, the output bounds are now calculated as follows:

$$\begin{aligned} &Y_k^{\min,\mathrm{int}} = \underline{Y^{\mathrm{r}}} - \psi(\underline{t}_k), \quad Y_k^{\max,\mathrm{int}} = \overline{Y^{\mathrm{r}}} + \psi(\underline{t}_k), \\ &Y_k^{\min,\mathrm{int}} \le y(t) \le Y_k^{\max,\mathrm{int}}, \quad \forall t \in [\underline{t}_k, \bar{t}_k + \tau_s/2), \\ &Y_k^{\min} = \underline{Y^{\mathrm{r}}} - \psi^{\mathrm{d}}(\bar{t}_k + \tau_{\mathrm{s}}/2), \; Y_k^{\max} = \overline{Y^{\mathrm{r}}} + \psi^{\mathrm{d}}(\bar{t}_k + \tau_{\mathrm{s}}/2), \\ &Y_k^{\min} \le y(t) \le Y_k^{\max}, \quad \forall t \in [\bar{t}_k + \tau_s/2, \underline{t}_{k+1}). \end{aligned}$$

The notation "int" indicates that it represents an intermediate value used to calculate $Z_k^{\max}$. We observe that $Y_k^{\max\,/\,\min,\mathrm{int}}$ depends on the adjusted funnel level $\psi(\underline{t}_k)$, which could potentially be large. In contrast, $Y_k^{\max\,/\,\min}$ depends only on $\psi^{\mathrm{d}}(t)$, thereby eliminating the influence of potentially large errors during the interval $[\underline{t}_k, \bar{t}_k + \tau_{\mathrm{s}}/2)$.

Furthermore, as shown in (43), if the interval between consecutive jumps is sufficiently long, the effect of the initial value—i.e., $Z_k^{\max,\mathrm{int}}$—will also diminish. This leads to a tighter bound for $\|z(t_{k+1}^-)\|$.

The remainder of the algorithm follows exactly as before. In Fig. 9, you can see the regions where we use to find an upper bound for $\|z(t_{k+1}^-)\|$.

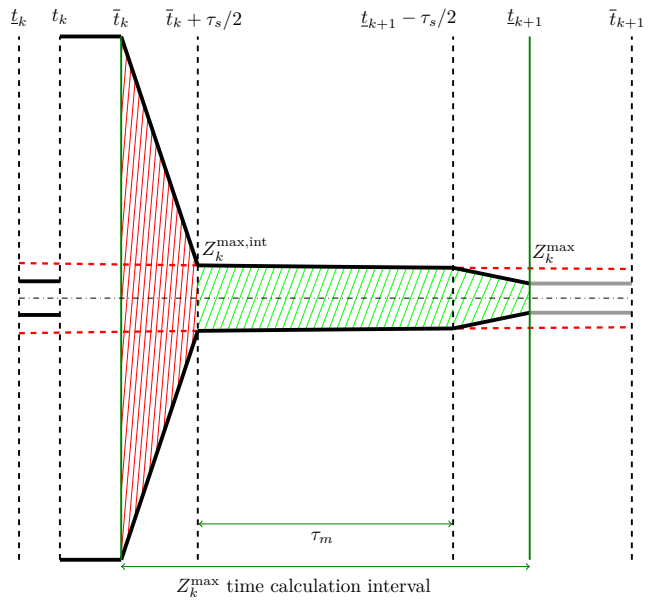

Figure 9: Calculation of the upper bound for $\|z_{k+1}^-\|$ in the interval $[\bar{t}_k, \underline{t}_{k+1})$ based on two sub-intervals: $[\bar{t}_k, \bar{t}_k + \tau_s/2)$ (red hatched area) and $[\bar{t}_k + \tau_s/2, \underline{t}_{k+1})$ (green hatched area).

To determine the Φ map in this case, we consider the Φ^{I} map of the mode. This map must be applied twice: first, over the interval $[\bar{t}_k, \bar{t}_k + \tau_s/2)$, and second, over the interval $[\bar{t}_k + \tau_s/2, \underline{t}_{k+1})$.

Suppose the dwell time of each mode is at least $\tau_s + \tau_m$, where τ_s is fixed and τ_m is mode-specific. Then, the duration of the interval $[\bar{t}_k, \bar{t}_k + \tau_s/2)$ is $\tau_s/2$, while the duration of the interval $[\bar{t}_k + \tau_s/2, \underline{t}_{k+1})$ is at least $\tau_m + \tau_s/2$. Therefore, we define:

$$\Phi_{\text{m}}^{\text{reset}}(z, \tau_s, \tau_m) = \beta_m\big(\Phi_{\text{m}}^{\text{I}}(z, \tau_s/2), \tau_m + \tau_s/2\big) + \gamma_m\big(\psi^{\text{d}}(\bar{t}_1 + \tau_s/2) + Y_{\max}^{\text{r}}\big) + c_m. \tag{44}$$

Notice that $\Phi_{\text{m}}^{\text{I}}(z, \tau_s/2)$ serves as the initial condition, equivalent to $Z_k^{\max,\text{int}}$. Moreover, since in $[\bar{t}_k + \tau_s/2, \underline{t}_{k+1})$ the upper bound of y depends only on the desired funnel, the largest value of $\psi^{\text{d}}(\bar{t}_k + \tau_s/2)$ for all k, i.e., $\psi^{\text{d}}(\bar{t}_1 + \tau_s/2)$ is used.

Similar to Φ^{B} and Φ^{I}, as long as Φ^{reset} is affine-bounded or affine-contractive, Theorem 4.4 can still be applied to determine whether the adjusted funnel remains bounded over time.

In the following, we numerically analyze the effect of resetting the calculation of $Z_k^{\max}$.

5.4. Numerical Example: $Z_k^{\max}$ Resetting

Example 2. Consider the following academic impulsive switched system.

Mode 1

$$\begin{aligned}
\dot{y}(t) &= z(t) + 0.2y(t) + u(t), && t \neq t_k,\\
y(t_k^+) &= \frac{1}{1 + e^{-y(t_k^-)}} + z(t_k^-) + y(t_k^-), && t = t_k,\\
\dot{z}(t) &= -0.7z(t) + y(t), && t \neq t_k,\\
z(t_k^+) &= 1.5z(t_k^-), && t = t_k.
\end{aligned}$$

Mode 2

$$\begin{aligned}
\dot{y}(t) &= -z(t) - 0.8y(t) + u(t), && t \neq t_k,\\
y(t_k^+) &= 2z(t_k^-) + y(t_k^-) + \begin{cases} 0.1 & \text{if } |y(t_k^-)| \leq 0.3,\\ 0.6 & \text{if } |y(t_k^-)| > 0.3 \end{cases}, && t = t_k,\\
\dot{z}(t) &= -0.5z(t) + y(t), && t \neq t_k,\\
z(t_k^+) &= 2.5z(t_k^-), && t = t_k.
\end{aligned}$$

Here, $y(0) = 0.7$, $z(0) = 0.5$, and $\|z(0)\| \in [0.2, 0.7]$. The desired funnel is given by $\psi^{\text{d}}(t) = 1.5e^{-0.07t} + 0.12$, with $\eta_k = \frac{1}{5}\psi^{\text{d}}(\bar{t}_k)$. The reference signal follows $y^{\text{r}}(t) = \sin(t) + 1$, where $\underline{Y^{\text{r}}} = 0$, $\overline{Y^{\text{r}}} = 2$, and $Y_{\max}^{\text{r}} = 2$. Also, $\eta_{\max} = \eta_1 = 0.25$. Mode 2 occurs first, with $\tau_1 = 6$, $\tau_2 = 11$, and $\tau_s = 3$. The mode transition follows $\underline{t}_{k+1} - \bar{t}_k = \tau_{\sigma_k} + \tau_s, \quad \forall k$. All jump uncertainty windows have a length of 1, starting from $t = 3$, with jumps occurring 0.4 seconds after $\underline{t}_k$. The bounds are:

Mode 1

$$\begin{aligned}
&\beta_1(\|z\|, t - t_k) = \|z(t_k^+)\|e^{-0.7(t-t_k)},\\
&\gamma_1(\|y\|_\infty) = 1.43\|y(t)\|_\infty,\ c_1 = 0,\ t \in [t_k, t_{k+1})\\
&\alpha_1(y, \|z\|) = 1 + \|z(t_k^-)\|,\ \alpha_1^{\text{z}}(y, \|z\|) = 2\|z(t_k^-)\|.
\end{aligned}$$

Mode 2

$$\begin{aligned}
&\beta_2(\|z\|, t - t_k) = \|z(t_k^+)\|e^{-0.5(t-t_k)},\\
&\gamma_2(\|y\|_\infty) = 2\|y(t)\|_\infty,\ c_2 = 0,\ t \in [t_k, t_{k+1})\\
&\alpha_2(y, \|z\|) = 0.6 + 2\|z(t_k^-)\|,\ \alpha_2^{\text{z}}(y, \|z\|) = 3\|z(t_k^-)\|.
\end{aligned}$$

First, we examine the case without resetting the calculation of $Z_k^{\max}$ to determine whether the upper bound of the jump height remains finite. To this end, Φ^{I} for the two modes is calculated as follows:

$$\begin{aligned}
\Phi_1^{\text{I}}(z, 9) &= 2e^{-0.7\times 9}z + 1.43(\max\{\eta_{\max} + 1 + z, 1.62\} + Y_{\max}^{\text{r}}),\\
&\leq 1.43z + 4.65,\\
\Phi_2^{\text{I}}(z, 14) &= 3e^{-0.5\times 14}z + 2(\max\{\eta_{\max} + 0.6 + 2z, 1.62\} + Y_{\max}^{\text{r}}),\\
&\leq 4.00z + 7.24.
\end{aligned}$$

Both λ values are greater than 1; therefore, the $Z_k^{\max}$ sequence and the jump height bounds will become unbounded if the calculation of $\|z(t)\|$ is not reset. Next,

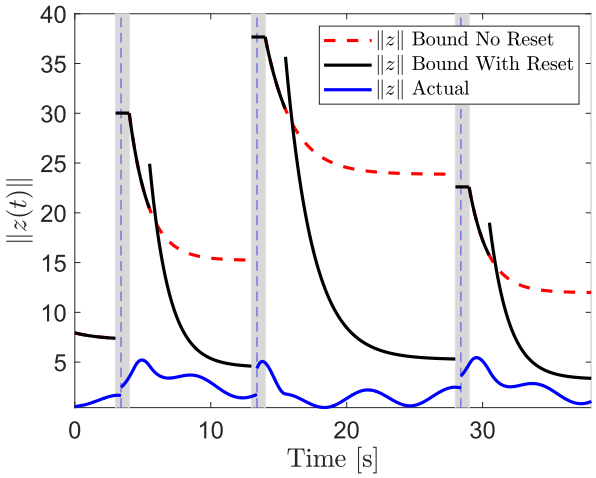

Figure 10: Evolution of $\|z(t)\|$ and its computed upper bounds for Example 2 with $Z_k^{\max}$ resetting. The red dashed line shows the bound on $\|z(t)\|$ if no reset had occurred at $\bar{t}_k + \tau_s/2$.

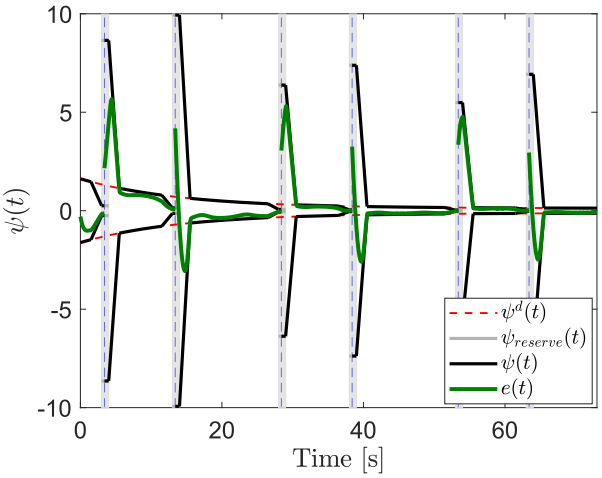

Figure 11: Adjusted funnel boundary and actual error evolution for Example 2 with $Z_k^{\max}$ resetting.

we calculate Φ^{reset},

$$\Phi_1^{\text{I}}(z, 1.5) = 2.13z + 4.65,$$
$$\Phi_1^{\text{reset}}(z, 3, 6) = (2.13z + 4.65)e^{-0.7\times 7.5} + 1.43(\psi^{\text{d}}(5.5) + Y_{\max}^{\text{r}}) = 0.01z + 4.52.$$
$$\Phi_2^{\text{I}}(z, 1.5) = 5.41z + 7.24,$$
$$\Phi_2^{\text{reset}}(z, 3, 11) = (5.41z + 7.24)e^{-0.5\times 12.5} + 2(\psi^{\text{d}}(5.5) + Y_{\max}^{\text{r}}) = 0.01z + 6.30.$$

Now, $\lambda_1\lambda_2 = 0.00$, which ensures that the $\|z(t)\|$ upper bound and the corresponding error jump bounds for the switched system remain bounded. In Figs. 10 and 11, the $\|z(t)\|$ upper bound and the resulting adjusted funnel boundary are illustrated. The red dashed line in Fig. 10 shows the bound on $\|z(t)\|$ without resetting at $\bar{t}_k + \tau_s/2$. With resetting, $\|z(t)\|$ exhibits a sudden increase at this instant, but this is compensated by the contribution of a much smaller bound on $y(t)$ from $\bar{t}_k + \tau_s/2$ onward, resulting in a significantly lower value at $\underline{t}_{k+1}$ compared to the red dashed line.

5.5. Impulse Time Sequence Design

A key advantage of having Practical ISS-stable internal states is the ability to design the impulse time sequence $\mathcal{T}$, when applicable, to ensure that the adjusted funnel remains bounded.

Specifically, given a time constant τ_s, τ_m can be designed for each mode to guarantee that the adjusted funnel remains bounded.

In other words, we can establish a lower bound on the time each mode persists before the next mode emerges. This ensures that the internal states have sufficient time to decrease, thereby preventing the escalation of the adjusted funnel boundary. The following theorem formalizes this property and provides the sufficient conditions for achieving this behavior.

Theorem 5.1. *Consider the system defined in (1) under assumptions **(S1)-(S3)**. Suppose prior information about the output and internal state jumps is given, as specified in **(J1)-(J2)**. Additionally, assume the reference signal and the desired funnel boundary satisfy assumptions **(P3)** and **(P1)**.*

Let a lower bound on the dwell time for each mode be denoted by $\tau_s + \tau_m$, where $\tau_s > 0$ is given and fixed across all modes, and $\tau_m \geq 0$ is mode-specific and to be determined. Define the set: $\tau = \{\tau_1, \tau_2, \ldots, \tau_M\}$, where M is the number of modes.

Suppose the internal states are Practical ISS-stable as defined in (9b). Assume that each mode m is associated with either the map $\Phi_m^{\text{I}}(z, \tau_s + \tau_m)$, as defined in (41), or the map $\Phi_m^{\text{reset}}(z, \tau_s, \tau_m)$, as defined in (44). Further, suppose these maps are $(\lambda_m(\tau_m), L_m(\tau_m))$-affine-bounded over $\mathcal{D}_m$ as in (25), in the sense of Definition 4.2.

Then, the adjusted funnel boundary computed by Algorithms 1–2 remains bounded for every time sequence τ that satisfies the following conditions:

$$\mathcal{S}_k(\tau) := \prod_{i=1}^{k} \lambda_{\sigma_i}(\tau_{\sigma_i}) < \infty,$$
$$\mathcal{C}_k(\tau) := \sum_{j=1}^{k} \left(\prod_{i=j+1}^{k} \lambda_{\sigma_i}(\tau_{\sigma_i}) \right) L_{\sigma_j}(\tau_{\sigma_j}) < \infty.$$

Proof. Define the set $\mathscr{T}$ as:

$$\mathscr{T} = \{\tau = \{\tau_1, \tau_2, \ldots, \tau_m\} \mid \mathcal{S}(\tau) < \infty,\ \mathcal{C}(\tau) < \infty\}.$$

For all $\tau \in \mathscr{T}$, the first and second conditions of Theorem 4.4 are satisfied. Consequently, the adjusted funnel boundary computed by Algorithms 1–2 remains bounded for every $\tau \in \mathscr{T}$. □

Although Theorem 5.1 provides sufficient conditions for the mode dwell-times to ensure a bounded adjusted funnel, finding such a set is not always straightforward. In these cases, we introduce a conservative yet computationally simple method to construct an impulse time sequence that is independent of the switching signal and guarantees a bounded adjusted funnel. This method is formalized in the following corollary.

Corollary 5.2. *Let* m^* *denote the mode with the slowest decay rate with respect to* Δt *among all maps* $\Phi^{\mathrm{I}}_{\mathrm{m}}(z, \Delta t)$. *Suppose that either* $\Phi^{\mathrm{I}}_{\mathrm{m}^*}(z, \tau_s + \tau_{\mathrm{m}^*})$ *or* $\Phi^{\mathrm{reset}}_{\mathrm{m}^*}(z, \tau_s, \tau_{\mathrm{m}^*})$ *is affine-bounded for every* $\tau_{\mathrm{m}^*} \geq 0$ *with parameters* $(\lambda_{\mathrm{m}^*}(\tau_{\mathrm{m}^*}), L_{\mathrm{m}^*}(\tau_{\mathrm{m}^*}))$. *Choose* τ_{m^*} *such that*

$$\lambda_{\mathrm{m}^*}(\tau_{\mathrm{m}^*}) < 1.$$

Then, for any arbitrary mode sequence $\{\sigma_k\}_{k\in\mathbb{N}_0}$, *the adjusted funnel remains bounded for all*

$$\tau = \{\tau_1, \tau_2, \ldots, \tau_{\mathrm{M}} \mid \tau_{\mathrm{m}} \leq \tau_{\mathrm{m}^*}, \forall \mathrm{m} \in \Sigma\}. \tag{45}$$

Proof. Let the mode m^* have the slowest decay rate, and suppose there exists a τ_{m^*} satisfying (45). Then, for all modes $\mathrm{m} \in \Sigma$, it holds that:

$$\tau_{\mathrm{m}} \leq \tau_{\mathrm{m}^*}, \quad \lambda_{\mathrm{m}}(\tau_{\mathrm{m}}) \leq \lambda_{\mathrm{m}^*}(\tau_{\mathrm{m}^*}).$$

Therefore, we derive:

$$\prod_{i=1}^{k} \lambda_{\sigma_i}(\tau_{\sigma_i}) \leq \prod_{i=1}^{k} \lambda_{\mathrm{m}^*}(\tau_{\mathrm{m}^*}) < 1,$$

and,

$$\sum_{j=1}^{k} \left(\prod_{i=j+1}^{k} \lambda_{\sigma_i}(\tau_{\sigma_i}) \right) L_{\sigma_j}(\tau_{\sigma_j}) \leq$$
$$\sum_{j=1}^{k} \lambda_{\mathrm{m}^*}(\tau_{\mathrm{m}^*})^{k-j} L_{\sigma_j}(\tau_{\sigma_j}) < \infty.$$

In the last inequality, since the geometric series

$$\sum_{k=1}^{\infty} \lambda_{\mathrm{m}^*}(\tau_{\mathrm{m}^*})^k$$

is convergent, it follows from Remark 4.5 that the entire series is bounded.

Therefore, $\mathcal{S}_k(\tau)$ and $\mathcal{C}_k(\tau)$ remain bounded as $k \to \infty$, ensuring the boundedness of the adjusted funnel. □

Remark 5.3. *For a single-mode system, define the set*

$$\mathscr{T} = \{\tau \in \mathbb{R}_{\geq 0} \mid \lambda(\tau) < 1\}.$$

Every $\tau \in \mathscr{T}$ *guarantees that the adjusted funnel boundary remains bounded.*

Remark 5.4. *For multi-mode systems with periodic switching signals, the adjusted funnel remains bounded for any dwell-time set*

$$\mathscr{T} = \left\{ \{\tau_1, \tau_2, \ldots, \tau_{\mathrm{M}}\} \,\middle|\, \prod_{\mathrm{m}=1}^{\mathrm{M}} \lambda_{\mathrm{m}}(\tau_{\mathrm{m}}) < 1 \right\}.$$

5.6. Numerical Example: Impulse Sequences Derivation

Let us determine a lower bound on the dwell times for modes 1 and 2 in Example 2 expressed in Section 5.4 that guarantees the adjusted funnel remains bounded. By recalculating $\Phi^{\mathrm{reset}}_{1/2}$ with $\tau_{\mathrm{s}} = 3$ while keeping τ_1 and τ_2 as parameters, the resulting expressions for $\lambda_1(\tau_1)$ and $\lambda_2(\tau_2)$ are given by:

$$\lambda_1(\tau_1) = 0.75e^{-0.7(\tau_1)}, \ \lambda_2(\tau_2) = 2.56e^{-0.5(\tau_2)}.$$

To ensure $\lambda_1(\tau_1)\lambda_2(\tau_2) < 1$, we multiply and simplify the inequality, yielding:

$$1.4\tau_1 + \tau_2 > 1.3. \tag{46}$$

Thus, any pair (τ_1, τ_2) satisfying (46) will necessarily result in a bounded adjusted funnel.

Note that L_1 and L_2 also depend on τ_1 and τ_2. However, for systems with periodic mode sequence, ensuring that $\lambda_1\lambda_2 < 1$ is sufficient to guarantee a bounded adjusted funnel, without requiring further conditions.

6. Additional Algorithm Enhancements

In this section, we explore further strategies to obtain tighter adjusted funnel boundaries. First, we consider asymmetric jump maps and refine Assumption **(J2)** accordingly. Next, we introduce level sets that cap the error in real time, preventing excessive growth, and illustrate their effect in a numerical example. Finally, we present an algorithm that adapts the adjusted funnel boundary online and demonstrate its effectiveness with another example.

6.1. Handling Asymmetric Jumps

In Assumption **(J2)**, the output jump height is assumed to be upper-bounded by the function α_{m}. However, if additional information about the jump maps is available—such as a lower bound for the jump that is different from $-\alpha_{\mathrm{m}}$—the resulting boundaries can be less conservative.

Therefore, we modify Assumption **(J2)** to account for the asymmetry in the bounds of error jumps.

(J2)′ Jump heights are presumed to be bounded by known smooth, possibly asymmetric functions $\underline{\alpha}_{\mathrm{m}}$ and $\overline{\alpha}_{\mathrm{m}}$. Specifically:

$$\underline{\alpha}_{\sigma_k}(y_k^-, z_k^-) \leq J_{\sigma_k}(y_k^-, \|z_k^-\|) - y_k^- \leq \overline{\alpha}_{\sigma_k}(y_k^-, z_k^-). \tag{10b}$$

As before, there is no requirement for the functions $\underline{\alpha}_{\mathrm{m}}$ and $\overline{\alpha}_{\mathrm{m}}$ to be the tightest bounds.

With the new assumption of **(J2)′**, the $y(t)$ bounds change to the following

$$Y_k^{\min,\mathrm{int}} = \underline{Y^{\mathrm{r}}} + \psi^-(\underline{t}_k), \ Y_k^{\max,\mathrm{int}} = \overline{Y^{\mathrm{r}}} + \psi^+(\underline{t}_k),$$
$$Y_k^{\min} = \underline{Y^{\mathrm{r}}} + \psi^{\mathrm{d}-}(\bar{t}_k + \tau_{\mathrm{s}}/2), Y_k^{\max} = \overline{Y^{\mathrm{r}}} + \psi^{\mathrm{d}+}(\bar{t}_k + \tau_{\mathrm{s}}/2).$$

Here, $\psi^-(t)$ and $\psi^+(t)$ represent the negative and positive funnel boundaries, respectively. Since the jump maps

are asymmetric, the resulting adjusted funnel may also be asymmetric. Additionally, $\psi^{\mathrm{d}-}(t)$ and $\psi^{\mathrm{d}+}(t)$ denote the negative and positive boundaries of the desired funnel, which may also be asymmetric.

$$C_k^{\min} := \inf_{\substack{y\in[-\eta_k+\underline{Y^{\mathrm{r}}},\eta_k+\overline{Y^{\mathrm{r}}}]\\ \|z\|\le Z_{k-1}^{\max}}} \underline{\alpha}_{\sigma_k}(y,\|z\|)$$

$$C_k^{\max} := \sup_{\substack{y\in[-\eta_k+\underline{Y^{\mathrm{r}}},\eta_k+\overline{Y^{\mathrm{r}}}]\\ \|z\|\le Z_{k-1}^{\max}}} \overline{\alpha}_{\sigma_k}(y,\|z\|)$$

The bounds of $e(t_{k+1}^+)$ also can be computed as:

$$E_k^{\min} = -\eta_k + C_k^{\min},\ E_k^{\max} = \eta_k + C_k^{\max}.$$

The rest of the algorithm remains unchanged. Moreover, the Φ maps are calculated as before. The only difference in this case is the existence of two maps: $\underline{\Phi}$, which is calculated based on $\underline{\alpha}$, and $\overline{\Phi}$, which is calculated based on $\overline{\alpha}$. To ensure a bounded adjusted funnel, the tests in Theorems 4.4 must be applied to both maps.

6.2. Adjusted Funnel Boundary Level Sets

The adjusted funnel boundaries achieved based on the presented method assume that the worst-case scenario always occurs. This means that, simultaneously, the jump heights of the output and internal states reach their maximum possible magnitudes, the reference signal attains its largest value between consecutive jumps, and the error before each jump equals the maximum allowable value, η_k. However, in reality, unless one is particularly unlucky, it is rare for all these worst-case conditions to occur, let alone simultaneously. Consequently, the actual error jumps are often much smaller than the computed adjusted boundaries.

Although even a significant difference between the funnel boundary and the actual error value does not destabilize the system, it may lead to undesired behaviors such as overshoots or undershoots, which could even exceed the error jump itself. Such behaviors are illustrated in Figs. 6 and 11.

One way to mitigate these effects is by precomputing level sets. Level sets are obtained by dividing the distance between the desired funnel and the adjusted funnel at $\bar{t}_k$ into n levels. When a jump in the error is detected, the nearest precomputed level is selected and becomes the active funnel boundary. Since the feedback gain is given by $k(t) = 1/(\psi(t) - |e(t)|)$, choosing the closest $\psi(t)$ to $e(t)$ (with at least an ε-margin) makes $k(t)$ immediately large, which prevents further error growth and drives it back toward lower levels.

Furthermore, detecting the direction of the jump allows the opposite side of the adjusted funnel to revert to the desired funnel, thereby preventing the error from crossing to the other side (see Fig. 11, second and fourth jumps).

Specifically, for each jump, given $E_k^{\min}$ and $E_k^{\max}$ already calculated based on Section 6.1, the following sets are defined:

$$E_k^{\ell,\min} = \left\{\psi^{\mathrm{d}+}(\bar{t}_k) + \tfrac{i}{n}\left(E_k^{\min} + \psi^{\mathrm{d}}(\bar{t}_k)\right) \,\middle|\, i = 0,\dots,n-1\right\},$$
$$E_k^{\ell,\max} = \left\{\psi^{\mathrm{d}-}(\bar{t}_k) + \tfrac{i}{n}\left(E_k^{\max} - \psi^{\mathrm{d}}(\bar{t}_k)\right) \,\middle|\, i = 0,\dots,n-1\right\}.$$

where $\psi^{\mathrm{d}+}$ and $\psi^{\mathrm{d}-}$ represent the positive and negative desired funnel boundaries, respectively.

Then, for each member of the sets, an adjusted funnel boundary is recomputed during the interval $[\underline{t}_k, \bar{t}_k + \tau_{\mathrm{s}}/2]$, based on Algorithm 1.

A key requirement for this improvement is the ability to detect jumps in real time. In the absence of a dedicated jump-detection device, or if there are delays in detecting jumps, an alternative is to monitor the error. If the error suddenly jumps out of the desired funnel boundary, it indicates that a jump has occurred.

6.3. Numerical Example: Asymmetric Jumps, Level Sets

In Example 2 (Section 5.4), instead of using $-\alpha$ and α for the bound on $|y_k^+ - y_k^-|$, the following output jump bounds are considered.

Mode 1: $\underline{\alpha}(\|z\|) = 0.5 + \|z\|, \quad \overline{\alpha}(\|z\|) = 1 + \|z\|.$
Mode 2: $\underline{\alpha}(\|z\|) = 0.1 - 2\|z\|, \overline{\alpha}(\|z\|) = 0.6 + 2\|z\|.$

$\overline{\Phi}_{1/2}^{\mathrm{reset}}$ remains the same as $\Phi_{1/2}^{\mathrm{reset}}$. However, $\underline{\Phi}_{1/2}^{\mathrm{reset}}$ must be recalculated based on $\underline{\alpha}_{1/2}$. Therefore,

$$\begin{aligned}\underline{\Phi}_1^I(z,9) &= 2e^{-0.7\times 9}z + 1.43|\min\{-\eta_{\max} + 0.5 + z, -1.62\} + 0|,\\ &\le 1.43z + 2.32.\\ \underline{\Phi}_2^I(z,14) &= 3e^{-0.5\times 14}z + 2|\min\{-\eta_{\max} + 0.1 - 2z, -1.62\} + 0|,\\ &\le 4.00z + 3.24.\end{aligned}$$

Next, we calculate $\underline{\Phi}_{1/2}^{\mathrm{reset}}$,

$$\begin{aligned}\underline{\Phi}_1^I(z,1.5) &= 2.13z + 2.32,\\ \underline{\Phi}_1^{\mathrm{reset}}(z,3,6) &= (2.13z + 2.32)e^{-0.7\times 7.5} + 1.43| - \psi^{\mathrm{d}}(5.5) + 0|,\\ &= 0.01z + 1.64.\\ \underline{\Phi}_2^I(z,1.5) &= 5.41z + 3.24,\\ \underline{\Phi}_2^{\mathrm{reset}}(z,3,11) &= (5.41z + 3.24)e^{-0.5\times 12.5} + 2| - \psi^{\mathrm{d}}(5.5) + 0|,\\ &= 0.01z + 2.29.\end{aligned}$$

$\underline{\Phi}_{1/2}^{\mathrm{reset}}$ suggests that $\underline{\psi}(t)$ remains bounded.

Additionally, to prevent undershoots (even jumps) and overshoots (odd jumps) in Fig. 11, we precompute ten level sets. Fig. 12 illustrates these precomputed adjusted funnel levels for all jumps, with the actual boundary used online shown in thick black. During the intervals $[\bar{t}_k + \frac{\tau_{\mathrm{s}}}{2}, \underline{t}_{k+1} - \frac{\tau_{\mathrm{s}}}{2}]$, all levels coincide with the desired funnel, since recovery occurs after $\bar{t}_k + \frac{\tau_{\mathrm{s}}}{2}$. As shown in Fig. 12, this strategy eliminates undershoots and overshoots. Moreover, the resulting boundaries are asymmetric, which is advantageous as it avoids unnecessary expansion of the adjusted funnel.

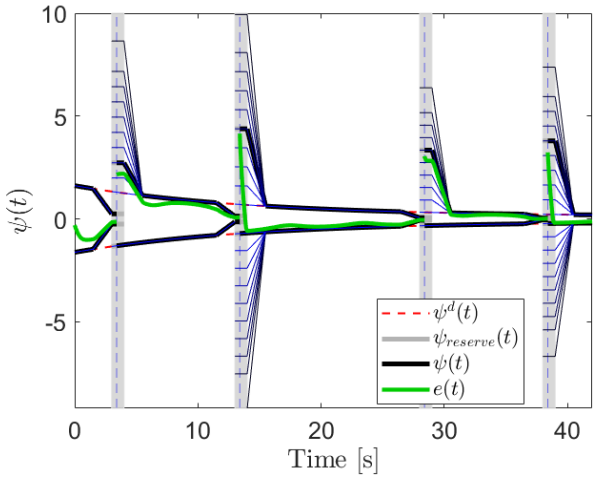

Figure 12: Precomputed level sets and the final adjusted funnel boundary (thick black line) based on the actual error jumps during online experiments for Example 2 with asymmetric jumps.

The tracking performance is also illustrated in Fig. 13. This figure shows small, smooth kinks in the output shortly after each jump. These arise from the abrupt change of the funnel boundary at $\bar{t}_k + \tau_s/2$ when it reverts to the desired funnel, which transiently bends the error (see Fig. 12 at the first and third jumps). A second source is error undershoot, which is clipped by the opposite side of the funnel, producing a similar short-lived bending (second and fourth jumps).

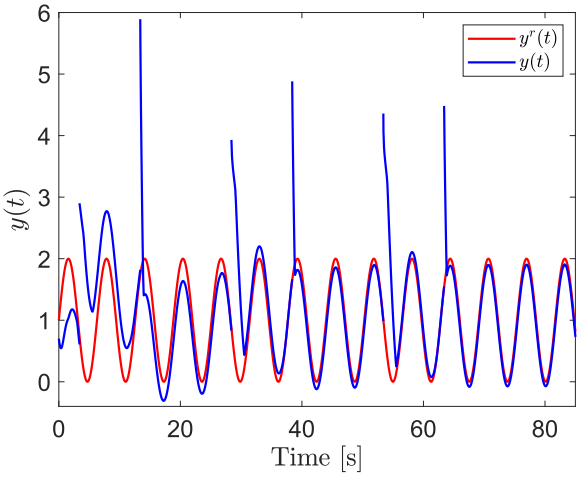

Figure 13: Tracking of $y^r(t)$ using the funnel controller for Example 2.

6.4. Real-Time Adjusted Funnel Boundary Update

Observations indicate that a decrease in $\|y_{[\underline{t}_k, \bar{t}_{k+1}]}\|_\infty$ leads to a lower upper bound for $\|z^-_{k+1}\|$, which in turn results in equal or smaller bounds for the next error jump. In other words, a smaller error jump height (reflected by a reduced $\|y_{[\underline{t}_k, \bar{t}_{k+1}]}\|_\infty$) decreases the bounds for subsequent jumps. Moreover, utilizing the actual $e(t)$ values allows us to modify the upper bounds of $\|z^+_k\|$, which further contributes to reducing the upper bound of $\|z^-_{k+1}\|$.

This observation can be exploited to reestablish the adjusted funnel boundaries during the experiment. Namely, instead of relying on the worst-case scenario for the error after the jump (i.e., the adjusted funnel boundary level), we can use the actual value of the error. Furthermore, having access to $y(t)$ allows us to determine the actual $\|y\|_\infty$ rather than its supremum.

The procedure for updating the adjusted funnel boundary at the kth jump, occurring at time $\underline{t}_k$, is presented in Algorithm 3. It is assumed that, after each jump, the closest level—maintaining at least an ε-distance from the error value—is selected from the predefined set of levels.

In short, the algorithm works as follows: first, $Z^{\max}_{k-1}$ is updated based on the actual values of $y(t)$ during $[t_{k-2}, t_{k-1}]$ (the optimal point for resetting is calculated to result in the minimum $Z^{\max}_{k-1}$). Then, based on the updated $Z^{\max}_{k-1}$ and the actual value of $y(t^-_{k-1})$, Z^+_{k-1} is updated. Next, using the updated Z^+_{k-1} and the actual values of $y(t)$ during $[t_{k-1}, \underline{t}_k]$, $Z^{\max}_k$ is updated (again, the optimal resetting point for the calculation of $Z^{\max}_k$ is determined and used). Finally, based on the updated value of $Z^{\max}_k$, E_k, which indicates the funnel level during $\mathcal{I}_k$, is updated.

It should be noted that the Φ_m maps will not change due to the online update of the adjusted funnel boundaries, unless experimental data provides a better approximation for the bounds of the internal states (β_m, γ_m, c_m), the output jump $(\underline{\alpha}_m, \overline{\alpha}_m)$, or the internal states jump (α^z_m).

6.5. Numerical Example: $\psi(t)$ Online Update

For Example 2 in Section 5.4, the adjusted funnel boundary is updated online based on Algorithm 3. The result is presented in Fig. 14. The final adjusted funnel boundary, incorporating online updates and the selection of the best level, is shown in Fig. 15.

7. Conclusion and Future Directions

This work proposed an adjusted funnel controller for nonlinear impulsive switched systems of relative degree one. The adjusted funnel boundary, computed offline and independent of system trajectories, contracts before jump windows and expands during them to ensure the tracking error remains within bounds.

By introducing maps that capture the interplay between internal states and output jumps, we derived sufficient conditions guaranteeing boundedness of the adjusted funnel boundary, along with quantitative bounds on the control input. Assuming Practical ISS rather than BIBO stability yielded tighter funnel bounds and quantitative bounds on dwell times. A resetting scheme for the internal-state bound further mitigated the effect of output jumps.

Algorithm 3: Real-Time Adjusted Funnel Update

Input : $t_{k-2}, t_{k-1}, y(t)\ \forall t \in [t_{k-2}, \underline{t}_k],\ k \in \mathbb{N}_{\geq 2}$; $\underline{t}_k, \overline{t}_k\ \forall k \in \mathbb{N}$

Output : $E_k^{\max}$, $E_k^{\min}$

For each $k \geq 2$**:**

Step 1: Update $Z_{k-1}^{\max}$ $(m = \sigma(t_{k-2}^+),\ t^* \in [t_{k-2}, t_{k-1}])$:

$$\tilde{Z}^{\text{int}}(t^*) := \beta_m(Z_{k-2}^+, t^* - t_{k-2}) + \gamma_m(\|y\|_{[t_{k-2}, t^*]}) + c_m,$$
$$\tilde{Z}(t^*) := \beta_m(\tilde{Z}^{\text{int}}(t^*), t_{k-1} - t^*) + \gamma_m(\|y\|_{[t^*, t_{k-1}]}) + c_m,$$
$$Z_{k-1}^{\max} := \min_{t^*} \tilde{Z}(t^*)$$

Step 2: Update Z_{k-1}^+

$$Z_{k-1}^+ := \sup_{\|z\| \leq Z_{k-1}^{\max}} \alpha^z_{\sigma(t_{k-1}^+)}(y(t_{k-1}^-), \|z\|)$$

Step 3: Update $Z_k^{\max}$ $(m = \sigma(t_{k-1}^+),\ t^* \in [t_{k-1}, \overline{t}_k))$:

$$Y_k^- := \max(|-\eta_k + \underline{Y^{\text{r}}}|, |\eta_k + \overline{Y^{\text{r}}}|),$$
$$\tilde{y}(t) := \begin{cases} y(t), & t \in [t_{k-1}, \underline{t}_k), \\ Y_k^-, & t \in [\underline{t}_k, \overline{t}_k), \end{cases}$$
$$\Delta t(t^*) := \begin{cases} \underline{t}_k - t^*, & t^* \in [t_{k-1}, \underline{t}_k), \\ \underline{t}_k - t_{k-1}, & t^* \in [\underline{t}_k, \overline{t}_k), \end{cases}$$
$$\tilde{Z}^{\text{int}}(t^*) := \beta_m(Z_{k-1}^+, t^* - t_{k-1}) + \gamma_m(\|y\|_{[t_{k-1}, t^*]}) + c_m,$$
$$\tilde{Z}(t^*) := \beta_m(\tilde{Z}^{\text{int}}(t^*), \Delta t(t^*)) + \gamma_m(\|y\|_{[t^*, \underline{t}_k]}) + c_m,$$
$$Z_k^{\max} := \min_{t^* \in [t_{k-1}, \underline{t}_k)} \tilde{Z}(t^*)$$

Step 4: Update error bounds:

$$E_k^{\max} = \eta_k + \sup_{\substack{y \in [-\eta_k + \underline{Y^{\text{r}}},\ \eta_k + \overline{Y^{\text{r}}}] \\ \|z\| \leq Z_k^{\max}}} \overline{\alpha}_{\sigma_k}(y, \|z\|),$$
$$E_k^{\min} = -\eta_k + \sup_{\substack{y \in [-\eta_k + \underline{Y^{\text{r}}},\ \eta_k + \overline{Y^{\text{r}}}] \\ \|z\| \leq Z_k^{\max}}} \underline{\alpha}_{\sigma_k}(y, \|z\|).$$

We also developed refinement strategies such as asymmetric jump map bounds, nearest-level selection, and dynamic online adjustments, each improving performance as confirmed by numerical examples.

Future work includes extending the approach to higher relative-degree systems and to interconnected hybrid systems with impulsive switching.

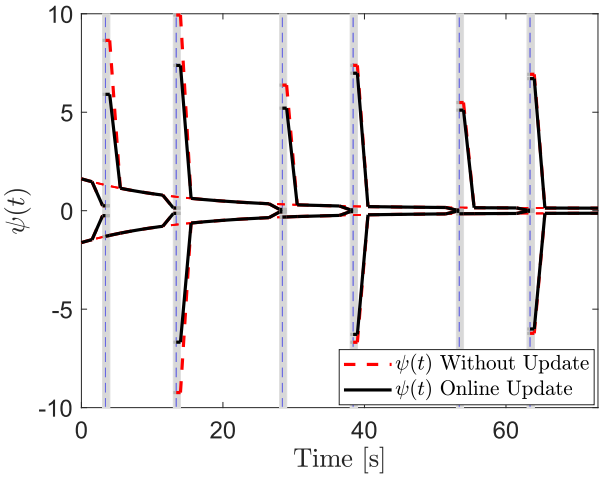

Figure 14: Adjusted funnel boundary with online updates compared to no updates for Example 2, with resetting of $Z_k^{\max}$ and asymmetric jumps.

References

[1] H. K. Khalil, Nonlinear Systems, 3rd Edition, Prentice Hall, Upper Saddle River, NJ, 2002.

[2] Y. Tang, X. Xing, H. R. Karimi, L. Kocarev, J. Kurths, Tracking control of networked multi-agent systems under new characterizations of impulses and its applications in robotic systems, IEEE Transactions on Industrial Electronics 63 (2) (2015) 1299–1307.

[3] X. Lu, N. Chen, Y. Wang, L. Qu, J. Lai, Distributed impulsive control for islanded microgrids with variable communication delays, IET Control Theory & Applications 10 (14) (2016) 1732–1739.

[4] W. Zhu, D. Wang, L. Liu, G. Feng, Event-based impulsive control of continuous-time dynamic systems and its application to synchronization of memristive neural networks, IEEE Transactions on Neural Networks and Learning Systems 29 (8) (2017) 3599–3609.

[5] Z.-W. Liu, G. Wen, X. Yu, Z.-H. Guan, T. Huang, Delayed impulsive control for consensus of multiagent systems with switching communication graphs, IEEE Transactions on Cybernetics 50 (7) (2019) 3045–3055.

[6] M. A. Nojoumian, M. R. Zakerzadeh, M. Ayati, Stabilization of delayed switched positive nonlinear systems under mode dependent average dwell time: A bumpless control scheme, Nonlinear Analysis: Hybrid Systems 47 (2023) 101300.

[7] M. A. Nojoumian, M. Ayati, M. R. Zakerzadeh, Bumpless stabilisation of uncertain switched positive linear systems under synchronous and asynchronous switching, International Journal of Systems Science 53 (2) (2022) 363–374.

[8] M. A. Nojoumian, M. Ayati, M. R. Zakerzadeh, Asynchronous bumpless stabilisation of uncertain switched linear positive systems with mixed time delay and l 1-gain performance, IET Control Theory & Applications 16 (2) (2022) 151–165.

[9] M. Babaali, M. Egerstedt, Observability of switched linear systems, in: Hybrid Systems: Computation and Control: 7th International Workshop, HSCC 2004, Philadelphia, PA, USA, March 25-27, 2004. Proceedings 7, Springer, 2004, pp. 48–63.

[10] P. S. Rivadeneira, C. H. Moog, Observability criteria for impulsive control systems with applications to biomedical engineering processes, Automatica 55 (2015) 125–131.

[11] N. Kalamian, H. Khaloozadeh, M. Ayati, Design of adaptive state-dependent impulsive observer for nonlinear time-delay systems, in: 2019 27th Iranian Conference on Electrical Engineering (ICEE), IEEE, 2019, pp. 885–890.

[12] M. Ayati, M. Alwan, X. Liu, H. Khaloozadeh, State estimation of stochastic impulsive system via stochastic adaptive impulsive observer, Asian Journal of Control 18 (2) (2016) 514–526.

[13] X. Li, P. Li, Q.-g. Wang, Input/output-to-state stability of impulsive switched systems, Systems & Control Letters 116 (2018) 1–7.

[14] A. Ilchmann, E. P. Ryan, C. J. Sangwin, Tracking with prescribed transient behaviour, ESAIM: Control, Optimisation and Calculus of Variations 7 (2002) 471–493.

[15] A. Ilchmann, E. P. Ryan, S. Trenn, Tracking control: Performance funnels and prescribed transient behaviour, Systems & Control Letters 54 (7) (2005) 655–670.

[16] T. Berger, H. H. Lê, T. Reis, Funnel control for nonlinear sys-

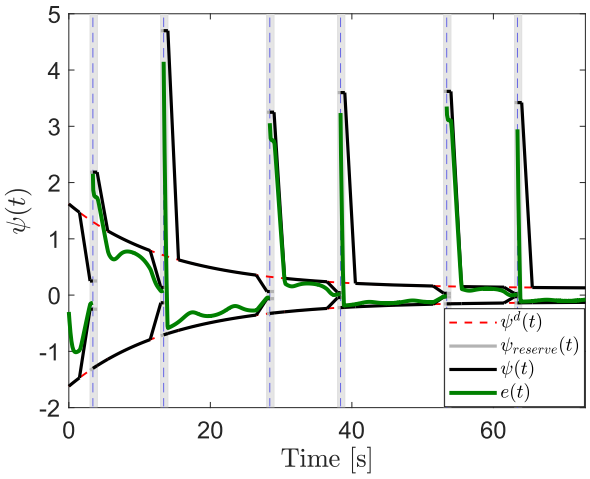

Figure 15: Adjusted funnel boundary and actual error evolution for Example 2 with online funnel updates, where the best level is selected after each jump.

tems with known strict relative degree, Automatica 87 (2018) 345–357.

[17] J. Hu, S. Trenn, X. Zhu, Funnel control for relative degree one nonlinear systems with input saturation, in: 2022 European Control Conference (ECC), IEEE, 2022, pp. 227–232.

[18] T. Berger, Input-constrained funnel control of nonlinear systems, IEEE Transactions on Automatic Control 69 (8) (2024) 5368–5382.

[19] T. Berger, Tracking with prescribed performance for linear non-minimum phase systems, Automatica 115 (2020) 108909.

[20] A. Hastir, J. J. Winkin, D. Dochain, Funnel control for a class of nonlinear infinite-dimensional systems, Automatica 152 (2023) 110964.

[21] J. G. Lee, T. Berger, S. Trenn, H. Shim, Edge-wise funnel output synchronization of heterogeneous agents with relative degree one, Automatica 156 (2023) 111204.

[22] J. G. Lee, T. Berger, S. Trenn, H. Shim, Utility of edge-wise funnel coupling for asymptotically solving distributed consensus optimization, in: 2020 European Control Conference (ECC), IEEE, 2020, pp. 911–916.

[23] X. Min, S. Baldi, W. Yu, J. Cao, Low-complexity control with funnel performance for uncertain nonlinear multiagent systems, IEEE Transactions on Automatic Control 69 (3) (2023) 1975–1982.

[24] X. Min, S. Baldi, W. Yu, J. Cao, Funnel asymptotic tracking of nonlinear multi-agent systems with unmatched uncertainties, Systems & Control Letters 167 (2022) 105313.

[25] T. Berger, A. Ilchmann, E. P. Ryan, Funnel control–a survey, arXiv preprint arXiv:2310.03449 (2023).

[26] S. Prajna, A. Jadbabaie, Safety verification of hybrid systems using barrier certificates, in: International workshop on hybrid systems: Computation and control, Springer, 2004, pp. 477–492.

[27] C. P. Bechlioulis, G. A. Rovithakis, A low-complexity global approximation-free control scheme with prescribed performance for unknown pure feedback systems, Automatica 50 (4) (2014) 1217–1226.

[28] Y. Li, S. Tong, L. Liu, G. Feng, Adaptive output-feedback control design with prescribed performance for switched nonlinear systems, Automatica 80 (2017) 225–231.

[29] A. K. Kostarigka, G. A. Rovithakis, Prescribed performance output feedback/observer-free robust adaptive control of uncertain systems using neural networks, IEEE Transactions on Systems, Man, and Cybernetics, Part B (Cybernetics) 41 (6) (2011) 1483–1494.

[30] T. Berger, L. Lanza, Funnel control of linear systems with arbitrary relative degree under output measurement losses, IMA Journal of Mathematical Control and Information 40 (4) (2023) 691–713.

[31] A. K. Pour, S. Trenn, Funnel control for impulsive switched systems, in: 2024 IEEE 63rd Conference on Decision and Control (CDC), IEEE, 2024, pp. 7810–7815.

[32] J. Hu, S. Trenn, X. Zhu, A novel two stages funnel controller limiting the error derivative, Systems & Control Letters 179 (2023) 105601.

[33] L. Lanza, D. Dennstädt, K. Worthmann, P. Schmitz, G. D. Şen, S. Trenn, M. Schaller, Sampled-data funnel control and its use for safe continual learning, Systems & Control Letters 192 (2024) 105892.

[34] D. D. Bonar, M. J. Khoury Jr, Real infinite series, Vol. 56, American Mathematical Soc., 2018.